

Oscillating neutrinos and $\mu \rightarrow e, \gamma$

J.A. Casas^{1*} and A. Ibarra^{1,2†}

¹ Instituto de Estructura de la Materia, CSIC
Serrano 123, 28006 Madrid

² Department of Physics, Theoretical Physics, University of Oxford
1 Keble Road, Oxford OX1 3NP, United Kingdom.

Abstract

If neutrino masses and mixings are suitable to explain the atmospheric and solar neutrino fluxes, this amounts to contributions to FCNC processes, in particular $\mu \rightarrow e, \gamma$. If the theory is supersymmetric and the origin of the masses is a see-saw mechanism, we show that the prediction for $\text{BR}(\mu \rightarrow e, \gamma)$ is in general larger than the experimental upper bound, especially if the largest Yukawa coupling is $\mathcal{O}(1)$ and the solar data are explained by a large angle MSW effect, which recent analyses suggest as the preferred scenario. Our analysis is bottom-up and completely general, i.e. it is based just on observable low-energy data. The work generalizes previous results of the literature, identifying the dominant contributions. Application of the results to scenarios with approximate top-neutrino unification, like SO(10) models, rules out most of them unless the leptonic Yukawa matrices satisfy very precise requirements. Other possible ways-out, like gauge mediated SUSY breaking, are also discussed.

March 2001

*E-mail: alberto@makoki.iem.csic.es

†E-mail: a.ibarra@physics.ox.ac.uk

1 Introduction

In the pure Standard Model, flavour is exactly conserved in the leptonic sector since one can always choose a basis in which the (charged) lepton Yukawa matrix, \mathbf{Y}_e , and gauge interactions are flavour-diagonal. If neutrinos are massive and mixed, as suggested by the observation of atmospheric and solar fluxes [1], this is no longer true and there exists a source of lepton flavour violation (LFV), in analogy with the Kobayashi–Maskawa mechanism in the quark sector. Unfortunately, due to the smallness of the neutrinos masses, the predicted branching ratios for these processes are so tiny that they are completely unobservable, namely $\text{BR}(\mu \rightarrow e\gamma) < 10^{-50}$ [2].

In a supersymmetric (SUSY) framework the situation is completely different. Besides the previous mechanism, supersymmetry provides new direct sources of flavour violation in the leptonic sector, namely the possible presence of off-diagonal soft terms in the slepton mass matrices $(m_L^2)_{ij}$, $(m_{e_R}^2)_{ij}$, and trilinear couplings A_{ij}^e [3]. There are in the literature very strong bounds on these matrix elements coming from requiring branching ratios for LFV processes to be below the experimental rates [4]. The strongest bounds come precisely from $\text{BR}(\mu \rightarrow e\gamma)$.

The most drastic way to avoid these dangerous off-diagonal terms is to impose perfect universality of the $(m_L^2)_{ij}$, $(m_{e_R}^2)_{ij}$, A_{ij}^e matrices, i.e. to take them proportional to the unit matrix. Then, of course, they maintain this form in any basis, in particular in the basis where all the gauge interactions and \mathbf{Y}_e are flavour-diagonal, so that we are left just with the previous tiny Kobayashi–Maskawa LFV effects. In principle, there is no theoretical reason to impose the universality constraint, and that is the so-called supersymmetric flavour problem. However, there are some particular supersymmetric scenarios, such as minimal supergravity, dilaton-dominated SUSY breaking or gauge-mediated SUSY breaking, that give rise to the desired universal soft terms (at least with much accuracy). In any case, the universality assumption is obviously the most conservative supposition that one can make about the form of the soft breaking terms when analyzing flavour violation effects; and this will be our starting point.

It turns out, however, that even under this extremely conservative assumption, if neutrinos are massive, radiative corrections may generate off-diagonal soft terms. The reason is that the flavour changing operators giving rise to the (non-diagonal) neutrino matrices will normally contribute to the renormalization group equations (RGEs) of

the $(m_L^2)_{ij}$, $(m_{e_R}^2)_{ij}$ and A_{ij}^e matrices, inducing off-diagonal entries.

The most interesting example of this occurs when neutrino masses are produced by a see-saw mechanism [5]. Then, above a certain scale M , there are new degrees of freedom, the right-handed neutrinos, which have conventional Yukawa couplings with a matricial Yukawa coupling \mathbf{Y}_ν . Normally, \mathbf{Y}_e and \mathbf{Y}_ν cannot be diagonalized simultaneously. Working in the flavour basis where \mathbf{Y}_e is diagonal, the off-diagonal entries of \mathbf{Y}_ν (more precisely, the off-diagonal entries of $\mathbf{Y}_\nu^+ \mathbf{Y}_\nu$) drive off-diagonal entries in the previous $(m_L^2)_{ij}$, and A_{ij}^e matrices through the RG running [6].

Actually, the supersymmetric see-saw is a extremely interesting scenario for a number of reasons. First, the see-saw mechanism is probably the most convincing and economical mechanism to naturally produce tiny neutrino masses (certainly it is the most popular one). Second, a *non*-supersymmetric see-saw suffers from a serious hierarchy problem. Perhaps this point has not been sufficiently acknowledged in the literature and we would like to emphasize it. It is common lore that the Standard Model (SM) presents a generic gauge hierarchy problem. Namely, the Higgs mass acquires quadratically-divergent radiative corrections, which, under the usual interpretation of the renormalization process, are naturally of the size of the scale at which new relevant physics enters. In a see-saw scenario the problem becomes more acute. The presence of very massive fermions (the right-handed neutrinos) coupled to the Higgs field produces logarithmically-divergent radiative corrections to the Higgs mass, which are proportional to M^2 . This can be immediately noticed from the usual expression of the 1-loop effective potential, where the neutrino mass eigenstates which are essentially right-handed neutrinos contribute as $\frac{1}{64\pi^2} M^2 Y_\nu^2 H^2 (\log \frac{M^2}{\mu^2} - \frac{3}{2}) + \dots$ (μ is the renormalization scale) [7]. In the supersymmetric framework, this problem is automatically cured by the presence of the right-handed sneutrinos with a similar mass. Consequently, it is fair to say that supersymmetry is the most natural arena to implement the see-saw mechanism.

This is precisely the scenario that we will consider in this paper, computing $\text{BR}(\mu \rightarrow e\gamma)$ in the most general case compatible with the observational (atmospheric and solar) indications about neutrino masses and mixing angles. This subject has been addressed in previous works, especially in refs. [8,9,10,11] (other related works can be found in ref.[12]). Let us briefly comment on the differences between the treatment of these works and the present one. The authors of ref.[8] adopt a “top-down” point of view,

i.e. they start with some sets of particular textures for \mathbf{Y}_e and \mathbf{Y}_ν , coming from more or less well motivated symmetries, e.g. family symmetries, which can produce sensible low-energy neutrino mass matrices, \mathcal{M}_ν , at the end of the day. Then, they study the corresponding predictions for $\text{BR}(\mu \rightarrow e\gamma)$. On the other hand, the authors of ref.[9,10,11] adopt a “bottom-up” point of view, i.e. they start with the experimental data about \mathcal{M}_ν at low energy, finding out a form of \mathbf{Y}_ν able to reproduce these data, and then computing the corresponding $\text{BR}(\mu \rightarrow e\gamma)$. Both approaches are interesting, but not general, as they are related to particular choices of \mathbf{Y}_ν . As a consequence, their results are not conclusive about what can we expect for $\text{BR}(\mu \rightarrow e\gamma)$ based on actual neutrino data. In our case, we also follow a “bottom-up” approach, i.e. we start with the existing experimental information about \mathcal{M}_ν . Then we find the *most general* textures for \mathbf{Y}_ν and \mathcal{M} (the Majorana mass matrix of the right-handed neutrinos) consistent with that information. In our opinion, this is by itself an interesting issue. The textures turn out to depend on some free parameters, but very few (as we shall see, the textures used in ref.[10] correspond to a particular choice for these parameters). Next, we compute $\text{BR}(\mu \rightarrow e\gamma)$ and compare it with present and forthcoming experimental bounds. The approach can be considered as a generalization of that by Hisano et al. in ref.[9,10]. As a matter of fact, we identify the dominant contributions, which were not considered in ref.[9,10] as a consequence of the particular texture used there.

The paper is organized as follows. In sect. 2 we determine the most general form of \mathbf{Y}_ν and $\mathbf{Y}_\nu^+\mathbf{Y}_\nu$, compatible with all the phenomenological requirements. In several subsections we specialize the general formulas previously obtained for relevant physical scenarios. In sect. 3 we review the way in which the RG-running induces off-diagonal terms, and the relevance of the latter for $l_i \rightarrow l_j, \gamma$ processes. In sect. 4 we apply the information of sects. 2, 3 to compute the predictions on $\text{BR}(l_i \rightarrow l_j, \gamma)$, with particular focus on $\text{BR}(\mu \rightarrow e, \gamma)$. These predictions can be understood analytically using some approximations, for the sake of clarity in the discussion. Again, in several subsections we present and discuss the results for different physical scenarios. In sect. 5 we offer a summary of the predictions on $\text{BR}(l_i \rightarrow l_j, \gamma)$ obtained in the previous sections. In sect. 6 we present our concluding remarks. Finally, we include an Appendix with the most important formulas that we have used for the full computations, specially RGEs and expressions for $\text{BR}(l_i \rightarrow l_j, \gamma)$.

2 General textures reproducing experimental data

The supersymmetric version of the see-saw mechanism has a superpotential

$$W = W_0 - \frac{1}{2} \nu_R^c T \mathcal{M} \nu_R^c + \nu_R^c T \mathbf{Y}_\nu L \cdot H_2, \quad (1)$$

where W_0 is the observable superpotential, except for neutrino masses, of the preferred version of the supersymmetric SM, e.g. the MSSM. The extra terms involve three additional neutrino chiral fields (one per generation; indices are suppressed) not charged under the SM group: ν_{Ri} ($i = e, \mu, \tau$). \mathbf{Y}_ν is the matrix of neutrino Yukawa couplings, L_i ($i = e, \mu, \tau$) are the left-handed lepton doublets and H_2 is the hypercharge $+1/2$ Higgs doublet. The Dirac mass matrix is given by $\mathbf{m}_D = \mathbf{Y}_\nu \langle H_2^0 \rangle$. Finally, \mathcal{M} is a 3×3 Majorana mass matrix which does not break the SM gauge symmetry. It is natural to assume that the overall scale of \mathcal{M} , which we will denote by M , is much larger than the electroweak scale or any soft mass. Below M the theory is governed by an effective superpotential

$$W_{eff} = W_0 + \frac{1}{2} (\mathbf{Y}_\nu L \cdot H_2)^T \mathcal{M}^{-1} (\mathbf{Y}_\nu L \cdot H_2), \quad (2)$$

obtained by integrating out the heavy neutrino fields in (1). The corresponding effective Lagrangian contains a mass term for the left-handed neutrinos:

$$\delta \mathcal{L} = -\frac{1}{2} \nu^T \mathcal{M}_\nu \nu + \text{h.c.}, \quad (3)$$

with

$$\mathcal{M}_\nu = \mathbf{m}_D^T \mathcal{M}^{-1} \mathbf{m}_D = \mathbf{Y}_\nu^T \mathcal{M}^{-1} \mathbf{Y}_\nu \langle H_2^0 \rangle^2, \quad (4)$$

suppressed with respect to the typical fermion masses by the inverse power of the large scale M . It is convenient to extract the Higgs VEV by defining the κ matrix as

$$\kappa = \mathcal{M}_\nu / \langle H_2^0 \rangle^2 = \mathbf{Y}_\nu^T \mathcal{M}^{-1} \mathbf{Y}_\nu, \quad (5)$$

where $\langle H_2^0 \rangle^2 = v_2^2 = v^2 \sin^2 \beta$ and $v = 174$ GeV. The experimental data about neutrino masses and mixings are referred to the \mathcal{M}_ν matrix, or equivalently κ , evaluated at low energy (electroweak scale). In this sense, it should be noted that eqs.(4, 5) are not defined at low energy but at the ‘‘Majorana scale’’, M . Therefore, in order to compare to the experiment one has still to run κ down to low energy through the corresponding

RGE². Alternatively, following the bottom-up spirit, one can start with the physical κ matrix at low energy and then run it upwards to the M scale, where eqs.(4, 5) are defined. This has been the procedure we have followed in all the numerical calculations to be presented in the next sections.

Working in the flavour basis in which the charged-lepton Yukawa matrix, \mathbf{Y}_e , and gauge interactions are flavour-diagonal, the κ matrix is diagonalized by the MNS [13] matrix U according to

$$U^T \kappa U = \text{diag}(\kappa_1, \kappa_2, \kappa_3) \equiv D_\kappa, \quad (6)$$

where U is a unitary matrix that relates flavour to mass eigenstates

$$\begin{pmatrix} \nu_e \\ \nu_\mu \\ \nu_\tau \end{pmatrix} = U \begin{pmatrix} \nu_1 \\ \nu_2 \\ \nu_3 \end{pmatrix}. \quad (7)$$

It is possible, and sometimes convenient, to choose $\kappa_i \geq 0$. Then, U can be written as

$$U = V \cdot \text{diag}(e^{-i\phi/2}, e^{-i\phi'/2}, 1) \quad , \quad (8)$$

where ϕ and ϕ' are CP violating phases (if different from 0 or π) and V has the ordinary form of a CKM matrix

$$V = \begin{pmatrix} c_{13}c_{12} & c_{13}s_{12} & s_{13}e^{-i\delta} \\ -c_{23}s_{12} - s_{23}s_{13}c_{12}e^{i\delta} & c_{23}c_{12} - s_{23}s_{13}s_{12}e^{i\delta} & s_{23}c_{13} \\ s_{23}s_{12} - c_{23}s_{13}c_{12}e^{i\delta} & -s_{23}c_{12} - c_{23}s_{13}s_{12}e^{i\delta} & c_{23}c_{13} \end{pmatrix}. \quad (9)$$

On the other hand, one can always choose to work in a basis of right neutrinos where \mathcal{M} is diagonal

$$\mathcal{M} = \text{diag}(\mathcal{M}_1, \mathcal{M}_2, \mathcal{M}_3) \equiv D_\mathcal{M}, \quad (10)$$

with $\mathcal{M}_i \geq 0$. Then, from eqs.(5, 6)

$$D_\kappa = U^T \mathbf{Y}_\nu^T D_{\mathcal{M}^{-1}} \mathbf{Y}_\nu U = U^T \mathbf{Y}_\nu^T D_{\sqrt{\mathcal{M}^{-1}}} D_{\sqrt{\mathcal{M}^{-1}}} \mathbf{Y}_\nu U \quad (11)$$

where, in an obvious notation, $D_{\sqrt{A}} \equiv +\sqrt{D_A}$. Multiplying both members of the eq.(11) by $D_{\sqrt{\kappa^{-1}}}$ from the left and from the right, we get

$$\mathbf{1} = \left[D_{\sqrt{\mathcal{M}^{-1}}} \mathbf{Y}_\nu U D_{\sqrt{\kappa^{-1}}} \right]^T \left[D_{\sqrt{\mathcal{M}^{-1}}} \mathbf{Y}_\nu U D_{\sqrt{\kappa^{-1}}} \right] \quad (12)$$

² For hierarchical neutrinos, with which we will be mainly concerned, this running does not substantially affect the texture of κ , and thus the mixing angles. It does modify, however, the overall size of κ , which has to be taken into account.

whose solution is $D_{\sqrt{\mathcal{M}^{-1}}}\mathbf{Y}_\nu U D_{\sqrt{\kappa^{-1}}} = R$, with R any orthogonal matrix (R can be complex provided $R^T R = \mathbf{1}$). Hence, in order to reproduce the physical, low-energy, parameters, i.e. the light neutrino masses (contained in D_κ) and mixing angles and CP phases (contained in U), the most general \mathbf{Y}_ν matrix is given by

$$\mathbf{Y}_\nu = D_{\sqrt{\mathcal{M}}} R D_{\sqrt{\kappa}} U^+ \quad (13)$$

So, besides the physical and measurable low-energy parameters contained in D_κ and U , \mathbf{Y}_ν depends on the three (unknown) positive mass eigenvalues of the righthanded neutrinos and on the three (unknown) complex parameters defining R . We will see, however, that in practical cases the number of relevant free parameters becomes drastically reduced. Let us stress that eq.(13), which is central for us, has to be understood at the M scale and in the above-defined basis, i.e. the flavour basis in which the charged-lepton Yukawa matrix, \mathbf{Y}_e , the right-handed Majorana mass matrix, \mathcal{M} , and the gauge interactions are flavour-diagonal. The extension of eq.(13) to other choices of basis is straightforward, taking into account the transformation properties of the \mathbf{Y}_e , \mathbf{Y}_ν , \mathcal{M} matrices under changes of basis. For example, if one works in a basis of ν_R where the \mathcal{M} matrix is non-diagonal, then the most general \mathbf{Y}_ν matrix reads $\mathbf{Y}_\nu = U_M^* D_{\sqrt{\mathcal{M}}} R D_{\sqrt{\kappa}} U^+$, where U_M is such that $\mathcal{M} = U_M^* D_{\mathcal{M}} U_M^+$. Let us also mention that eq.(13) is valid as well for the non-supersymmetric see-saw mechanism.

As commented in sect. 1, in ref.[10] a particular choice for \mathbf{Y}_ν was taken, which corresponds to take $R = \mathbf{1}$ in eq.(13). This is equivalent to assume that there exists a basis of L_i and ν_{Ri} in which \mathbf{Y}_ν and \mathcal{M} are simultaneously diagonal (though not \mathbf{Y}_e). To see this notice that if $R = \mathbf{1}$, then \mathbf{Y}_ν , as given by eq.(13), can be made diagonal by rotating L_i with the U -matrix. This hypothesis may be consistent with certain models, namely when all the leptonic flavour violation can be attributed to the sector of charged leptons, but clearly it is not general, and it is inconsistent with other scenarios.

Another special choice of R occurs when the \mathbf{Y}_ν matrix given by eq.(13) has the form $\mathbf{Y}_\nu = W D_Y$, where D_Y is a diagonal matrix and W is a unitary matrix. From the see-saw formula (5), W is related to $D_{\mathcal{M}}$ and D_Y through $D_{\sqrt{\mathcal{M}^{-1}}} = W^* (D_{Y^{-1}\kappa} D_{Y^{-1}}) W^+$. Then, by rotating ν_{Ri} with the W -matrix, \mathbf{Y}_e and \mathbf{Y}_ν get simultaneously diagonal, while \mathcal{M} gets non-diagonal, more precisely $\mathcal{M} = D_Y \kappa^{-1} D_Y$. In other words, all the leptonic flavour violation can be attributed to the sector of right-handed neutrinos, in

contrast to the previous situation. It is important to remark that both are very special situations, not generic at all.

On the other hand, as we will see in the next section, the rate for $l_i \rightarrow l_j, \gamma$ processes just depends on the $\mathbf{Y}_\nu^+ \mathbf{Y}_\nu$ matrix (to be precise, on the matrix element $(\mathbf{Y}_\nu^+ \mathbf{Y}_\nu)_{ij}$) rather than on \mathbf{Y}_ν , since this is the quantity that enters the RGEs of the off-diagonal soft parameters. From eq.(13) $\mathbf{Y}_\nu^+ \mathbf{Y}_\nu$ has the general form

$$\mathbf{Y}_\nu^+ \mathbf{Y}_\nu = U D_{\sqrt{\kappa}} R^+ D_{\mathcal{M}} R D_{\sqrt{\kappa}} U^+ \quad (14)$$

Notice that $\mathbf{Y}_\nu^+ \mathbf{Y}_\nu$, and therefore eq.(14), do not depend on the ν_R -basis, and thus on the fact that \mathcal{M} is diagonal or not.

In order to illustrate the use of eqs.(13, 14), let us consider some interesting scenarios that often appear in the literature

2.1 ν_L 's and ν_R 's completely hierarchical

In this case $\kappa_1 \ll \kappa_2 \ll \kappa_3$ and $\mathcal{M}_1 \ll \mathcal{M}_2 \ll \mathcal{M}_3$, so that D_κ and $D_{\mathcal{M}}$ can be approximated by

$$D_\kappa \simeq \text{diag}(0, \kappa_2, \kappa_3), \quad D_{\mathcal{M}} \simeq \text{diag}(0, 0, \mathcal{M}_3) \quad (15)$$

where $(v_2^2 \kappa_2)^2 \simeq (\Delta m_\nu^2)_{sol}$, $(v_2^2 \kappa_3)^2 \simeq (\Delta m_\nu^2)_{atm}$. Then, from eq.(13),

$$(\mathbf{Y}_\nu)_{ij} \simeq \sqrt{\mathcal{M}_3} \delta_{i3} R_{3l} \sqrt{\kappa_l} U_{lj}^+ \quad (16)$$

So, for a certain set of low-energy physical quantities (given by κ_l and U), \mathbf{Y}_ν just depends on two (generally complex) parameters, $\sqrt{\mathcal{M}_3} R_{32}$ and $\sqrt{\mathcal{M}_3} R_{33}$. Let us remark that, although the $(\mathbf{Y}_\nu)_{1j}$ and $(\mathbf{Y}_\nu)_{2j}$ entries are proportional to $\sqrt{\mathcal{M}_1}$ and $\sqrt{\mathcal{M}_2}$ respectively, and thus suppressed, they are normally relevant if one wishes to reconstruct the neutrino mass matrix, κ , from \mathbf{Y}_ν , $D_{\mathcal{M}}$ through the see-saw equation (5). Still, they are *not* relevant for the $\mathbf{Y}_\nu^+ \mathbf{Y}_\nu$ entries, and thus for the predictions on $\text{BR}(l_i \rightarrow l_j, \gamma)$, which is our main goal.

It is interesting to notice that this scenario also includes the possibility of an ‘‘inverse hierarchy’’, i.e. $\sim \text{diag}(\mathcal{M}_3, 0, 0)$, or any other ordering. The reason is that one can permute the entries of $D_{\mathcal{M}}$ by redefining the ν_R 's through an appropriate rotation. In particular, one can pass from an inverse hierarchy to an ordinary one through a rotation in the 1-3 ‘‘plane’’: $\nu_R = R_p \nu'_R$ with $R_p = \{(0, 0, 1), (0, 1, 0), (-1, 0, 0)\}$. Then,

$\mathbf{Y}_\nu \rightarrow \mathbf{Y}'_\nu = D'_{\sqrt{\mathcal{M}}} R_p^T R D_{\sqrt{\kappa}} U^+$ with $D'_{\mathcal{M}} = R_p^T D_{\mathcal{M}} R_p$. Hence, the general formula (13) and its particularization (16) remain identical with the modification $R \rightarrow R' = R_p^T R$. Since R runs over all possible orthogonal matrices, so R' does. So, both starting points (inverse or ordinary hierarchy) lead to the same complete results.

In many models one can impose an extra condition coming from the unification of Yukawa couplings. In particular, in simple $SO(10)$ models, usually one of the $\mathbf{Y}_\nu^+ \mathbf{Y}_\nu$ eigenvalues (the largest one) coincides with the top Yukawa coupling $|Y_t|^2$ at the unification scale, M_X (in other more elaborate models, it coincides with $3|Y_t|^2$) [14]. We will denote $|Y_0|^2$ this maximum eigenvalue. Now, from eq.(16), the largest eigenvalue of $\mathbf{Y}_\nu^+ \mathbf{Y}_\nu$ is $|Y_0|^2 \simeq \mathcal{M}_3 (|R_{32}|^2 \kappa_2 + |R_{33}|^2 \kappa_3)$, which (after running up to M_X) would be identified with $|Y_t(M_X)|^2$. This eliminates one real parameter, leaving just R_{33}/R_{32} , plus one phase, e.g. $\text{phase}(R_{33})$, as the independent parameters. Actually, as mentioned above, the $l_i \rightarrow l_j, \gamma$ processes just depends on the $\mathbf{Y}_\nu^+ \mathbf{Y}_\nu$ matrix, which does not depend on the previous phase. Therefore, one is just left with one (complex) parameter, R_{33}/R_{32} .

A convenient way to visualize this is to take the following parametrization³ of R

$$R = \begin{pmatrix} \hat{c}_2 \hat{c}_3 & -\hat{c}_1 \hat{s}_3 - \hat{s}_1 \hat{s}_2 \hat{c}_3 & \hat{s}_1 \hat{s}_3 - \hat{c}_1 \hat{s}_2 \hat{c}_3 \\ \hat{c}_2 \hat{s}_3 & \hat{c}_1 \hat{c}_3 - \hat{s}_1 \hat{s}_2 \hat{s}_3 & -\hat{s}_1 \hat{c}_3 - \hat{c}_1 \hat{s}_2 \hat{s}_3 \\ \hat{s}_2 & \hat{s}_1 \hat{c}_2 & \hat{c}_1 \hat{c}_2 \end{pmatrix}, \quad (17)$$

where $\hat{\theta}_1, \hat{\theta}_2, \hat{\theta}_3$ are arbitrary complex angles. Then, from eq.(16)

$$\mathbf{Y}_\nu \simeq \frac{|Y_0|}{\sqrt{(|\hat{s}_1|^2 \kappa_2 + |\hat{c}_1|^2 \kappa_3)}} \frac{\hat{c}_2}{|\hat{c}_2|} \times \begin{pmatrix} \hat{\theta} & 0 & 0 \\ 0 & 0 & 0 \\ \hat{s}_1 \sqrt{\kappa_2} U_{12}^* + \hat{c}_1 \sqrt{\kappa_3} U_{13}^* & \hat{s}_1 \sqrt{\kappa_2} U_{22}^* + \hat{c}_1 \sqrt{\kappa_3} U_{23}^* & \hat{s}_1 \sqrt{\kappa_2} U_{32}^* + \hat{c}_1 \sqrt{\kappa_3} U_{33}^* \end{pmatrix} \quad (18)$$

which depends just on the angle $\hat{\theta}_1$ and the phase $\frac{\hat{c}_2}{|\hat{c}_2|}$; $\mathbf{Y}_\nu^+ \mathbf{Y}_\nu$ depends just on $\hat{\theta}_1$. The previous equation should be understood at the \mathcal{M} scale; the prefactor $|Y_0|$ represents the square root of the maximal eigenvalue of $\mathbf{Y}_\nu^+ \mathbf{Y}_\nu$ at the \mathcal{M} -scale.

In the typical case in which everything is real, very used in the literature, the $\hat{\theta}_i$ angles are real, and hence \mathbf{Y}_ν and $\mathbf{Y}_\nu^+ \mathbf{Y}_\nu$ depend on a single real parameter, $\hat{\theta}_1$.

³The parametrization (17) does not count all the possible forms of R , as it does not include ‘‘reflections’’. However, for the scenario considered in this subsection it is general enough, since the uncounted forms of R do not produce different textures of \mathbf{Y}_ν .

Therefore, in spite of the additional degrees of freedom introduced by the lack of knowledge about R , this scenario is quite predictive.

In the previous discussion, it has been assumed that at least one of the two entries, R_{32} or R_{33} , is different from zero. However, it may happen that $R_{32} = R_{33} = 0$. Then, κ_1 , \mathcal{M}_1 , \mathcal{M}_2 cannot be neglected anymore in the general equation eq.(13). It is worth-noticing that going to the basis where the $D_{\mathcal{M}}$ matrix is ‘inverse hierarchical’, i.e. $\nu_R \rightarrow R_p \nu_R$, $D_{\mathcal{M}} \rightarrow \text{diag}(\mathcal{M}_3, \mathcal{M}_2, \mathcal{M}_1)$, this possibility translates into $R_{12} = R_{13} = 0$, which includes the particularly simple case $R = \mathbf{1}$.

2.2 ν_L ’s hierarchical and ν_R ’s degenerate

In this case, D_{κ} and $D_{\mathcal{M}}$ have the form

$$D_{\kappa} \simeq \text{diag}(0, \kappa_2, \kappa_3), \quad D_{\mathcal{M}} \simeq \text{diag}(\mathcal{M}, \mathcal{M}, \mathcal{M}) \quad (19)$$

where, again, $(v_2^2 \kappa_2)^2 \simeq (\Delta m^2)_{sol}$, $(v_2^2 \kappa_3)^2 \simeq (\Delta m^2)_{atm}$. Then, from eq.(13),

$$(\mathbf{Y}_{\nu})_{ij} \simeq \sqrt{\mathcal{M}} R_{il} \sqrt{\kappa_l} U_{lj}^+ \quad (20)$$

So, in principle, for a certain set of low-energy physical quantities (given by κ_q and U), \mathbf{Y}_{ν} depends on one real parameter (\mathcal{M}) and three complex ones defining the R matrix. Notice, however, that in the real case, where $R^+ = R^T$, $\mathbf{Y}_{\nu}^+ \mathbf{Y}_{\nu}$ takes the simple form

$$\mathbf{Y}_{\nu}^+ \mathbf{Y}_{\nu} = \mathcal{M} U D_{\kappa} U^+ , \quad (21)$$

which just contains one free parameter, \mathcal{M} . This can be fixed by a unification condition, similarly to the previous case. Here $|Y_0|^2 \simeq \mathcal{M} \kappa_3 \simeq |Y_t|^2$ (where the identification must be understood at the M_X scale). Therefore, this is also a very predictive scenario. Notice that here $\mathbf{Y}_{\nu}^+ \mathbf{Y}_{\nu}$ does not depend on the form of R , so in this case the choice $R = \mathbf{1}$ is indeed general enough to study $l_i \rightarrow l_j, \gamma$ processes.

2.3 ν_L ’s quasi-degenerate

In this case $D_{\kappa} \simeq \text{diag}(\kappa_1, \kappa_2, \kappa_3)$, with $\kappa_1 \sim \kappa_2 \sim \kappa_3 \equiv \kappa$. Then, it is logical to assume that \mathcal{M} has degenerate eigenvalues, otherwise a big conspiracy would be needed between \mathbf{Y}_{ν} and \mathcal{M} so that $\kappa_1 \sim \kappa_2 \sim \kappa_3$ in eq.(5). Hence

$$D_{\kappa} \simeq \text{diag}(\kappa, \kappa, \kappa), \quad D_{\mathcal{M}} \simeq \text{diag}(\mathcal{M}, \mathcal{M}, \mathcal{M}) . \quad (22)$$

Consequently, eq.(20) and eq.(21) (for R real) hold in this case too. Since $D_\kappa \simeq \kappa \mathbf{1}$, from eq.(21) we notice

$$\mathbf{Y}_\nu^+ \mathbf{Y}_\nu = \mathcal{M} U D_\kappa U^+ \simeq |Y_0|^2 \mathbf{1} , \quad (23)$$

where $|Y_0|^2 = \mathcal{M} \kappa_3$ is the largest eigenvalue of the $\mathbf{Y}_\nu^+ \mathbf{Y}_\nu$ matrix. This means that for quasi-degenerate neutrinos, with R real, we expect small off-diagonal entries in $\mathbf{Y}_\nu^+ \mathbf{Y}_\nu$ and thus suppressed $l_i \rightarrow l_j, \gamma$ rates. We will be more quantitative about the size of those entries in subsect. 4.3.

The scenario of partially degenerate neutrinos will also be addressed in that section.

3 RG-induced lepton flavour violating soft terms and $l_i \rightarrow l_j, \gamma$

In addition to the supersymmetric Lagrangian, which contains the gauge interactions plus the part derived from the superpotential (1), one has to consider the soft breaking terms (gaugino and scalar masses, and trilinear and bilinear scalar terms) coming from the (unknown) supersymmetry breaking mechanism. In a self-explanatory notation, they have the form

$$- \mathcal{L}_{\text{soft}} = \left(m_L^2\right)_{ij} \bar{L}_i L_j + \left(m_{e_R}^2\right)_{ij} \bar{e}_{Ri} e_{Rj} + \left(A_{eij} e_{Ri}^c H_1 L_j + \text{h.c.}\right) + \text{etc.} , \quad (24)$$

where we have written explicitly just the soft breaking terms in the leptonic sector, namely scalar masses and trilinear scalar terms. All the fields in the previous equation denote just the corresponding scalar components. As explained in sect. 1, concerning flavour violation the most conservative starting point for $\mathcal{L}_{\text{soft}}$ is the assumption of universality, which corresponds to take

$$\left(m_L^2\right)_{ij} = m_0^2 \mathbf{1}, \quad \left(m_{e_R}^2\right)_{ij} = m_0^2 \mathbf{1}, \quad A_{eij} = A_0 \mathbf{Y}_{eij} , \quad (25)$$

so that working in the L_i and e_{Ri} basis where \mathbf{Y}_e is diagonal, the soft terms do not contain off-diagonal (lepton flavour violating) entries.

As mentioned in sect. 1, this is only strictly true at the scale where universality is imposed, e.g. M_X in GUT models. Below that scale, the RGEs of the soft terms, which contain non-diagonal contributions proportional to $\mathbf{Y}_\nu^+ \mathbf{Y}_\nu$, induce off-diagonal

soft terms⁴. These contributions are decoupled at the characteristic scale of the right-handed neutrinos, M . As noted e.g. in ref. [6], and as it is clear from eqs.(67–71) in the Appendix, this mechanism is not efficient to generate off-diagonal entries in the $(m_{e_R}^2)$ matrix, since the corresponding RGE does not contain $\sim \mathbf{Y}_\nu^+ \mathbf{Y}_\nu$ terms. More precisely, in the leading-log approximation⁵, the off-diagonal soft terms at low-energy are given by

$$\begin{aligned} (m_L^2)_{ij} &\simeq \frac{-1}{8\pi^2} (3m_0^2 + A_0^2) (\mathbf{Y}_\nu^+ \mathbf{Y}_\nu)_{ij} \log \frac{M_X}{M}, \\ (m_{e_R}^2)_{ij} &\simeq 0, \\ (A_e)_{ij} &\simeq \frac{-3}{8\pi^2} A_0 Y_{l_i} (\mathbf{Y}_\nu^+ \mathbf{Y}_\nu)_{ij} \log \frac{M_X}{M}, \end{aligned} \quad (26)$$

where $i \neq j$ and Y_{l_i} is the Yukawa coupling of the charged lepton l_i .

The amplitude for a $l_i \rightarrow l_j, \gamma$ process has the general form

$$T = \epsilon^\alpha \bar{l}_j m_{l_i} i \sigma_{\alpha\beta} q^\beta (A_L P_L + A_R P_R) l_i, \quad (27)$$

where q is the momentum of the photon, $P_{RL} = (1 \pm \gamma_5)/2$ and A_L (A_R) is the coefficient of the amplitude when the incoming l_i lepton is left (right), and thus the l_j lepton is right (left). The expressions for A_L , A_R can be found in the literature [9] (see Appendix for more details). The corresponding branching ratio is given by

$$\text{BR}(l_i \rightarrow l_j, \gamma) = \frac{12\pi^2}{G_F^2} (|A_L|^2 + |A_R|^2) \quad (28)$$

Notice that the $l_i \rightarrow l_j, \gamma$ process violates the chiral symmetries $l_{Rk} \rightarrow e^{i\alpha_k} l_{Rk}$. Under the assumption of initial universality, this symmetry is violated just by the Yukawa coupling of the corresponding lepton. Thus, A_L (A_R) is proportional to the mass of the righthanded lepton involved, i.e. l_{jR} (l_{iR}). Since $m_{l_j}^2 \ll m_{l_i}^2$, then $|A_L|^2 \ll |A_R|^2$. This can also be checked by inspection of the diagrams that contribute to $l_i \rightarrow l_j, \gamma$, taking into account eq.(26). It is interesting to note that the angular distribution of l_j with respect to the polarization direction of the incoming lepton (P_{l_i}) depends on the relative magnitudes of the coefficients A_L , A_R . The relation $|A_L|^2 \ll |A_R|^2$ predicted

⁴We will pay attention just to the contribution that appears in the MSSM, i.e. the one $\propto \mathbf{Y}_\nu^+ \mathbf{Y}_\nu$. This is a minimal possibility. In more complicated models, there can be additional sources of flavour violation in the RGEs, leading to larger predictions for $\text{BR}(l_i \rightarrow l_j, \gamma)$.

⁵We use the leading-log approximation through the text in order to make the results easily understandable. Nevertheless, the numerical results, to be exposed below, have been obtained by integrating the full set of RGEs.

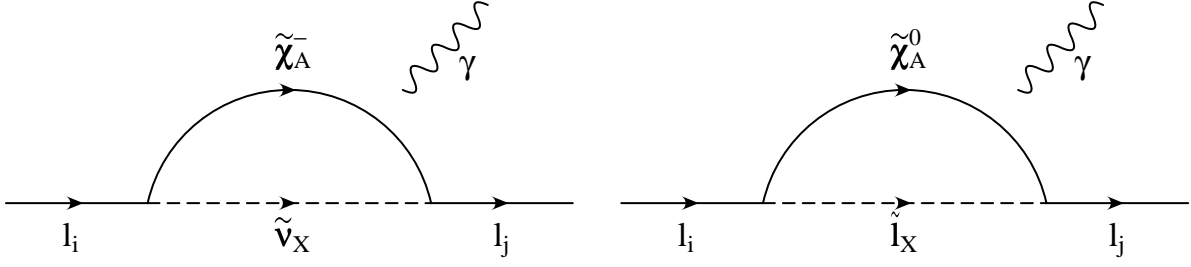


Figure 1: Feynman diagrams contributing to $l_i \rightarrow l_j, \gamma$. $\tilde{\nu}_X$ and \tilde{l}_X with $X = 1, \dots, 3$ ($4, \dots, 6$) represent the mass eigenstates of “left” (“right”) sneutrinos and charged sleptons, respectively. $\tilde{\chi}_A^-$, $A = 1, 2$, denote the charginos, whereas $\tilde{\chi}_A^0$, $A = 1, \dots, 4$, denote the neutralinos.

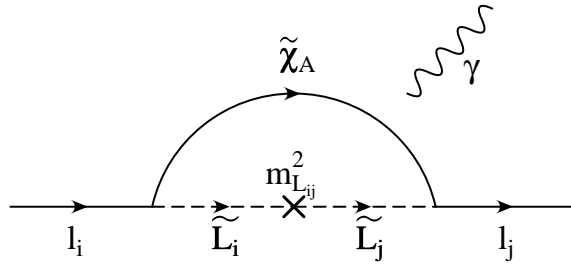


Figure 2: Dominant Feynman diagrams contributing to $l_i \rightarrow l_j, \gamma$ in the mass-insertion approximation. \tilde{L}_i are the slepton doublets in the basis where the gauge interactions and the charged-lepton Yukawa couplings are flavour-diagonal. $\tilde{\chi}_A$ denote the charginos and neutralinos, as in Fig. 1.

by the see-saw mechanism, and which does not hold in general in other models of generation of neutrino masses, gives a characteristic $(1 - P_i \cos \theta)$ distribution that could be measured by future experiments [15].

We have taken into account all contributions to $\text{BR}(l_i \rightarrow l_j, \gamma)$, using the general expressions given in the literature, in particular from ref. [9], as explained in the Appendix. These have not been obtained by using the mass-insertion approximation, but by diagonalizing all the mass matrices involved in the task, i.e. those of (left and right) sleptons, charginos and neutralinos. The diagrams have the form shown in Fig. 1. The precise form of $\text{BR}(l_i \rightarrow l_j, \gamma)$ that we have used in our computations is a rather cumbersome expression, given in the Appendix. However, for the sake of the physical discussion it is interesting to think in the mass-insertion approximation to identify the dominant contributions. As discussed in ref. [10], these correspond to the mass-insertion diagrams enhanced by $\tan \beta$ factors. All of them are proportional to $m_{L_{ij}}^2$, and have the generic form shown in Fig. 2. So, in all cases

$$\text{BR}(l_i \rightarrow l_j, \gamma) \simeq \frac{12\pi^2}{G_F^2} |A_R|^2 \sim \frac{\alpha^3}{G_F^2} \frac{|m_{Lij}^2|^2}{m_S^8} \tan^2 \beta, \quad (29)$$

where m_S^2 represents supersymmetric leptonic scalar masses.

From eq.(29) it is clear that $\text{BR}(l_i \rightarrow l_j, \gamma)$ depends crucially on the quantity m_{Lij}^2 , which at low energy is given by the integration of its RGE, as explained above. In the scenario examined in this paper (i.e. supersymmetric see-saw), and in the leading-log approximation, $m_{Lij}^2 \propto (\mathbf{Y}_\nu^+ \mathbf{Y}_\nu)_{ij}$, as given by eq.(26), so

$$\text{BR}(l_i \rightarrow l_j, \gamma) \sim \frac{\alpha^3}{G_F^2 m_S^8} \left| \frac{-1}{8\pi^2} (3m_0^2 + A_0^2) \log \frac{M_X}{M} \right|^2 |(\mathbf{Y}_\nu^+ \mathbf{Y}_\nu)_{ij}|^2 \tan^2 \beta \quad (30)$$

The $\mathbf{Y}_\nu^+ \mathbf{Y}_\nu$ matrix, which is therefore the crucial quantity, has been evaluated in sect. 2 in the general and in particular cases. Next, we apply those results to the computation of $\text{BR}(l_i \rightarrow l_j, \gamma)$,

4 Experimental data on neutrinos and predictions for $\text{BR}(l_i \rightarrow l_j, \gamma)$

We study here the expectable predictions for $l_i \rightarrow l_j, \gamma$ from the existing experimental information on neutrinos. Let us mention that the present and forthcoming experimental bounds on $l_i \rightarrow l_j, \gamma$ make $\mu \rightarrow e, \gamma$ the process with higher potential to constrain theories involving flavour violation. The present limit is $\text{BR}(\mu \rightarrow e, \gamma) < 1.2 \times 10^{-11}$ [16] and it is going to improve in the near future (year 2003) until $\sim 10^{-14}$ [17]. Hence, we will pay special attention to $\mu \rightarrow e, \gamma$. Nevertheless, as we will see, other processes like $\tau \rightarrow \mu, \gamma$ and $\tau \rightarrow e, \gamma$ offer information complementary to that from $\mu \rightarrow e, \gamma$, which in some cases can be extremely important. For $\tau \rightarrow \mu, \gamma$, in particular, the present (future) upper limit is 1.1×10^{-6} ($\sim 10^{-9}$) [18,19]. Finally, there exist interesting limits on other branching ratios, like $\text{BR}(\mu \rightarrow eee) < 10^{-12}$ and $\text{BR}(\mu Ti \rightarrow e Ti) < 6 \times 10^{-13}$ [20,21]. The latter is also to improve in projected experiments [22]. These limits are certainly very small, but the theoretical predictions on the branching ratios are also much smaller due to the presence of extra electromagnetic vertices [23]

From the results of the previous section, namely eq.(30), we know that $\text{BR}(l_i \rightarrow l_j, \gamma) \propto |(\mathbf{Y}_\nu^+ \mathbf{Y}_\nu)_{ij}|^2$. On the other hand, from the general equation (14), it is clear that the matrix element $(\mathbf{Y}_\nu^+ \mathbf{Y}_\nu)_{ij}$ will depend on several facts: the low-energy spectrum of

neutrinos (contained in D_κ), the neutrino mixing angles (contained in U), the right-handed neutrino spectrum (contained in $D_{\mathcal{M}}$) and the choice of the R matrix. Let us discuss them in order.

The experimental (solar and atmospheric) data [1] strongly suggest a hierarchy of neutrino mass-splittings, $\Delta\kappa_{sol}^2 \ll \Delta\kappa_{atm}^2$. Numerically, $\Delta\kappa_{atm}^2 \simeq (1.4 - 6.1) \times 10^{-3} \text{eV}^2/v_2^4$ [24] (with central value around $3 \times 10^{-3} \text{eV}^2/v_2^4$), while the value of $\Delta\kappa_{sol}^2$ depends on the solution considered to explain the solar neutrino problem [25,26]. The most favoured one from the recent analyses of data [24] is the large-angle MSW solution (LAMSW), which requires $\Delta\kappa_{sol}^2 \sim 3 \times 10^{-5} \text{eV}^2/v_2^4$. Other solutions are (in order of reliability from these analyses) the LOW MSW-solution, the small angle MSW-solution (SAMSW) and the vacuum oscillations solution (VO). They require, in eV^2/v_2^4 units, $\Delta\kappa_{sol}^2 \sim 10^{-7}$, 5×10^{-6} and 8×10^{-10} respectively. The corresponding uncertainties are discussed e.g. in ref.[24]. In any case, there are basically three types of neutrino spectra consistent with the hierarchy of mass-splittings [27]: *hierarchical* ($\kappa_1^2 \ll \kappa_2^2 \ll \kappa_3^2$), *“intermediate”* ($\kappa_1^2 \sim \kappa_2^2 \gg \kappa_3^2$) and *“degenerate”* ($\kappa_1^2 \sim \kappa_2^2 \sim \kappa_3^2$). We follow the usual notation in which κ_3 corresponds to the most split mass eigenvalue, so that $\Delta\kappa_{atm}^2 \equiv \Delta\kappa_{32}^2$, $\Delta\kappa_{sol}^2 \equiv \Delta\kappa_{21}^2$.

The hierarchical scenario seems perhaps the most natural one, since it resembles the other fermion spectra. Indeed, it is the natural spectrum in GUT theories, particularly $SO(10)$ models. In any case, it is the most extensively analyzed scenario in the literature and we will pay special attention to it. In this scenario one should take $\kappa_3^2 \simeq \Delta\kappa_{atm}^2$, $\kappa_2^2 \simeq \Delta\kappa_{sol}^2$, $\kappa_1^2 \simeq 0$. The other two scenarios (intermediate and degenerate) are also interesting and we will address them. In particular, the degenerate scenario is the only one compatible with a relevant cosmological role of neutrinos (provided $\kappa \simeq \mathcal{O}(1)\text{eV}/v_2^2$).

Concerning the mixing angles, θ_{23} and θ_{13} are constrained by the atmospheric and CHOOZ data to be near maximal and minimal, respectively. The θ_{12} angle depends on the solution considered to explain the solar neutrino problem. In the LAMSW case, θ_{12} is near maximal. In the other explanations of the solar neutrino problem θ_{12} can be either minimal (SAMSW), or near maximal (VO and LOW). The precise preferred values for the angles depend on the sets of data used in the fits. For example, from the global analysis of ref.[24] these are $\tan^2 \theta_{13} \sim 0.005$, $\tan^2 \theta_{23} \sim 1.4$ and, for the LAMSW, $\tan^2 \theta_{12} \sim 0.36$. The uncertainties depend also on the type of fit, as well as

on the values used for the mass splittings. In summary, the two basic forms that U can present are either a single-maximal or (more plausibly) a bimaximal mixing matrix. Schematically,

$$U \sim \begin{pmatrix} 1 & 0 & 0 \\ 0 & \frac{1}{\sqrt{2}} & \frac{1}{\sqrt{2}} \\ 0 & -\frac{1}{\sqrt{2}} & \frac{1}{\sqrt{2}} \end{pmatrix} \quad \text{or} \quad U \sim \begin{pmatrix} \frac{1}{\sqrt{2}} & \frac{1}{\sqrt{2}} & 0 \\ -\frac{1}{2} & \frac{1}{2} & \frac{1}{\sqrt{2}} \\ \frac{1}{2} & -\frac{1}{2} & \frac{1}{\sqrt{2}} \end{pmatrix}, \quad (31)$$

With regard to the spectrum of right-handed neutrinos, there are two basic possibilities: either they are hierarchical, i.e. $\mathcal{M}_1 \ll \mathcal{M}_2 \ll \mathcal{M}_3$, or they are degenerate, i.e. $\mathcal{M}_1 \sim \mathcal{M}_2 \sim \mathcal{M}_3$. Both of them were considered in sect. 2, where it was also shown that the first possibility counts the case of an ‘‘inverse hierarchy’’ or any other ordering of the \mathcal{M} eigenvalues.

Finally, R is the generic (complex) orthogonal matrix discussed in sect. 2. In principle, it contains three independent complex parameters, but we saw that this number can be usually reduced in a drastic way.

Let us analyze now the predictions for $\text{BR}(l_i \rightarrow l_j, \gamma)$ in the different scenarios above exposed.

4.1 ν_L 's and ν_R 's completely hierarchical

4.1.1 The generic case

We consider first the case where both the left-handed and the right-handed neutrinos are completely hierarchical, i.e.

$$D_\kappa \simeq \text{diag}(0, \kappa_2, \kappa_3), \quad D_{\mathcal{M}} \simeq \text{diag}(0, 0, \mathcal{M}_3). \quad (32)$$

We are neglecting for the moment contributions of $\mathcal{O}(\mathcal{M}_2)$. (Later on, we will discuss when those contributions would be relevant.) The general form of the \mathbf{Y}_ν matrix in this case was already worked out in subsect. 2.1. If $R_{32} \neq 0$ or $R_{33} \neq 0$ (later on we will consider the case $R_{32}, R_{33} \simeq 0$), \mathbf{Y}_ν is given by eq.(16), so only the last row of \mathbf{Y}_ν has sizeable entries. Thus, the relevant quantity $(\mathbf{Y}_\nu^+ \mathbf{Y}_\nu)_{ij}$ has the form

$$(\mathbf{Y}_\nu^+ \mathbf{Y}_\nu)_{ij} = (\mathbf{Y}_\nu)_{3i}^* (\mathbf{Y}_\nu)_{3j} = \mathcal{M}_3 \left[\sum_{l=2,3} R_{3l}^* \sqrt{\kappa_l} U_{il} \right] \left[\sum_{l'=2,3} R_{3l'} \sqrt{\kappa_{l'}} U_{j'l'}^* \right] \quad (33)$$

Focusing on $\mu \rightarrow e, \gamma$, and using the parametrization of R of eq.(17), eq.(30) reads

$$\begin{aligned} \text{BR}(\mu \rightarrow e, \gamma) &\propto \left| (\mathbf{Y}_\nu^+ \mathbf{Y}_\nu)_{21} \right|^2 \\ &= \left| \mathcal{M}_3 |\hat{c}_2|^2 [\hat{s}_1^* \sqrt{\kappa_2} U_{22} + \hat{c}_1^* \sqrt{\kappa_3} U_{23}] [\hat{s}_1 \sqrt{\kappa_2} U_{12}^* + \hat{c}_1 \sqrt{\kappa_3} U_{13}^*] \right|^2 \end{aligned} \quad (34)$$

Let us recall here that, since κ_2 and κ_3 represent the solar and atmospheric splitting, respectively, then $\kappa_2 \ll \kappa_3$. Also, the matrix element $U_{13} \sim s_{13} \ll 1$, as θ_{13} is the mixing angle constrained by CHOOZ. In the SAMSW scenario, U_{12} and U_{23} are also extremely small (see eq.(9)), so $\mu \rightarrow e, \gamma$ is suppressed. However, in the other scenarios (LAMSW, VO and LOW) U is basically a bimaximal mixing matrix. Then $U_{12}, U_{23} \simeq 1/\sqrt{2}$, $U_{22} \simeq 1/2$. Let us recall that this precisely includes the scenarios favoured from present data, i.e. LAMSW and LOW.

The prefactor $\mathcal{M}_3|\hat{c}_2|^2$ in eq.(30) can be written as

$$\mathcal{M}_3|\hat{c}_2|^2 = \frac{|Y_0|^2}{|\hat{s}_1|^2\kappa_2 + |\hat{c}_1|^2\kappa_3} \quad (35)$$

where $|Y_0|^2$ is the largest eigenvalue of $(\mathbf{Y}_\nu^+\mathbf{Y}_\nu)$. So, the right hand side of eq.(34) depends just on two independent parameters, $|Y_0|^2$ and $\hat{\theta}_1$ (the remaining parameters have a precise physical meaning and are measurable at low energy). If we further impose a unification condition, like $|Y_0(M_X)| = |Y_t(M_X)|$, $\text{BR}(\mu \rightarrow e, \gamma)$ depends just on one parameter, $\hat{\theta}_1$. This conclusion could also be obtained from eq.(18).

Now, as discussed in sect. 2, the results of ref. [10] correspond to take $R = \mathbf{1}$, i.e. $\hat{c}_i = 1$. Then, $\text{BR}(\mu \rightarrow e, \gamma)$, as written in eq.(34) is suppressed by $|U_{13}|^2 \ll 1$. The authors of ref.[10] considered however the contributions of $\mathcal{O}(\mathcal{M}_2)$ (which we have not considered yet). Then, working in the LAMSW scenario, they obtained a non-vanishing result for $\text{BR}(\mu \rightarrow e, \gamma)$, as a function of \mathcal{M}_2 . What is apparent from eqs.(34, 35) is that that result corresponds to a very special point in the parameter space, namely $\hat{c}_1 = 1$. In general, $\hat{c}_1 \neq 1, \hat{s}_1 \neq 0$, so the prediction for $\text{BR}(\mu \rightarrow e, \gamma)$ is much larger. For random values of $\hat{\theta}_1$ we expect

$$(\mathbf{Y}_\nu^+\mathbf{Y}_\nu)_{21} \sim \frac{|Y_0|^2}{|\hat{s}_1|^2\kappa_2 + |\hat{c}_1|^2\kappa_3} \hat{c}_1^* \hat{s}_1 \sqrt{\kappa_3\kappa_2} U_{23} U_{12}^* \quad (36)$$

This formula allows to compare the foreseeable predictions for $\text{BR}(\mu \rightarrow e, \gamma)$ in different scenarios, taking into account the different values for κ_2, U_{ij} . Clearly, the largest values for $\text{BR}(\mu \rightarrow e, \gamma)$ are obtained for the LAMSW scenario (precisely, the most favoured one by the present analyses). For the LOW and SAMSW scenarios one expects predictions ~ 20 and ~ 1000 times smaller respectively. Indeed, for the LAMSW scenario the previous equation generically gives a branching ratio above the *present* experimental limits, at least for $Y_0 = \mathcal{O}(1)$, as it occurs in the unified scenarios!

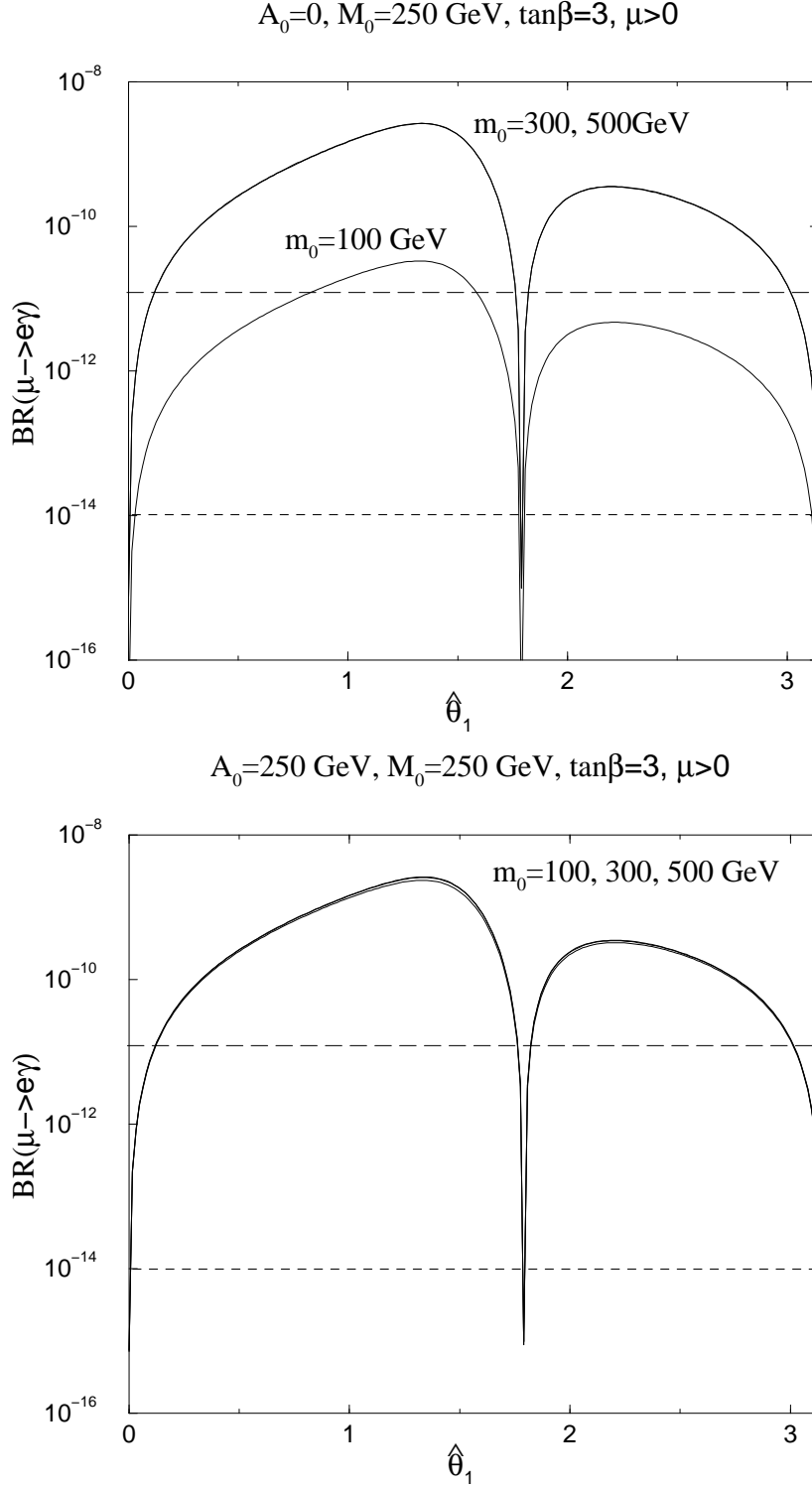


Figure 3: Branching ratio of the process $\mu \rightarrow e, \gamma$ vs. the unknown angle $\hat{\theta}_1$ for the case of hierarchical (left and right) neutrinos and two typical sets of supersymmetric parameters, as indicated in the plots. The dashed lines correspond to the present and forthcoming upper bounds. A top-neutrino “unification” condition has been used to fix the value of the largest neutrino Yukawa coupling at high energy. $\hat{\theta}_1$ is taken real for simplicity, so the two limits $\hat{\theta}_1 = 0, \pi$ of the horizontal axis represent the same physical point. In the upper plot the curves corresponding to $m_0 = 300 \text{ GeV}$ and $m_0 = 500 \text{ GeV}$ are almost indistinguishable. The same is true in the lower plot for the curves corresponding to $m_0 = 100 \text{ GeV}$, $m_0 = 300 \text{ GeV}$ and $m_0 = 500 \text{ GeV}$.

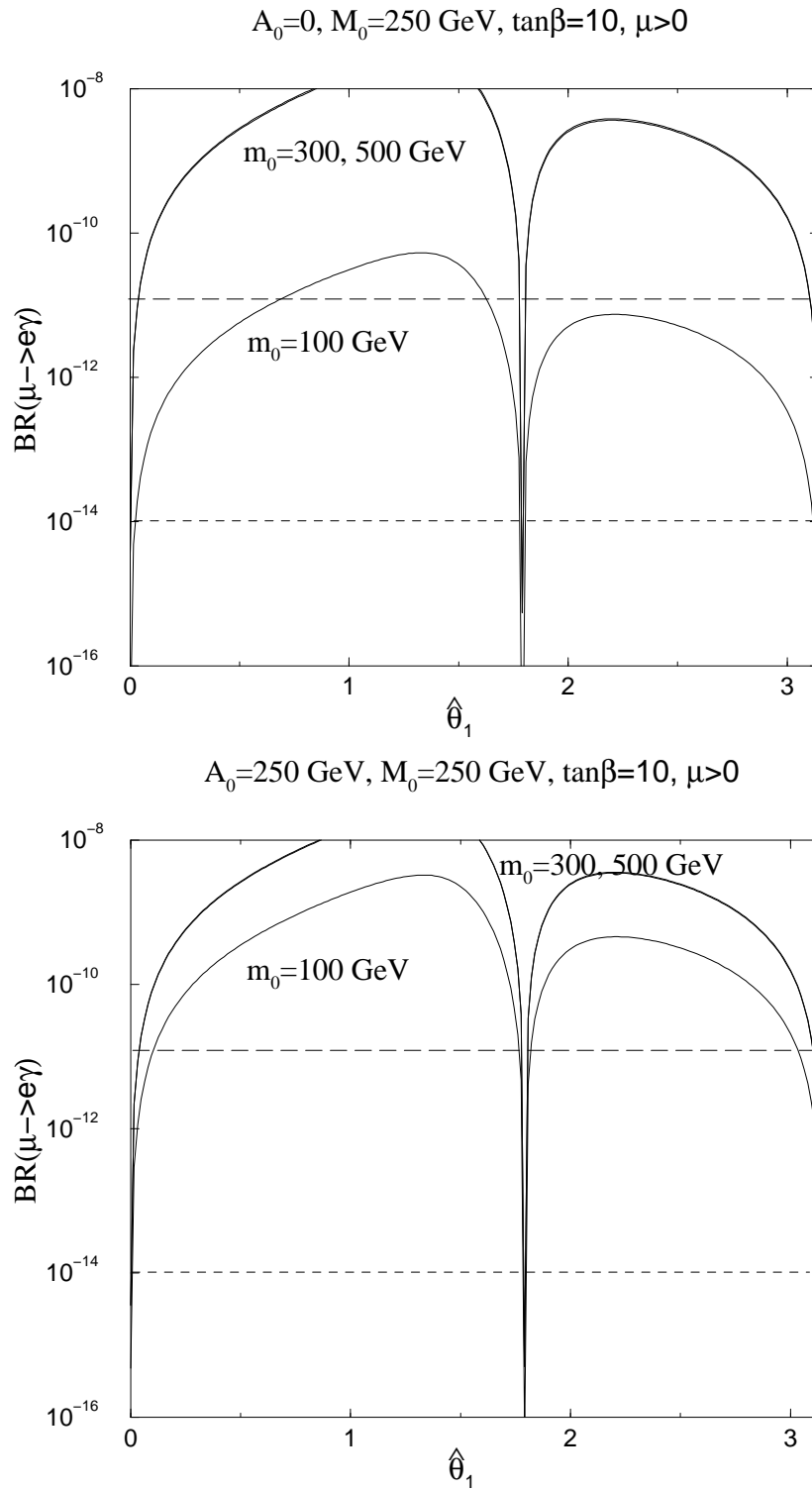


Figure 4: The same as Fig. 3, but for $\tan\beta = 10$.

This is apparent from the plots of Fig. 3, where it is shown $\text{BR}(\mu \rightarrow e, \gamma)$ vs. $\hat{\theta}_1$ in the LAMSW scenario for different typical sets of supersymmetric parameters, using a unification condition for the largest neutrino Yukawa coupling, i.e. $|Y_0(M_X)|^2 = |Y_t(M_X)|^2$, with $M_X = 2 \times 10^{16}$ GeV. Incidentally, the value of the supersymmetric μ -parameter is extracted (here and throughout the paper) from the electroweak breaking condition, choosing $\mu > 0$. We have not shown the results for $\mu < 0$ since they are always very similar. From Fig. 3, it is clear that most of the parameter space (i.e. the range of $\hat{\theta}_1$) is already excluded by the present bounds on $\text{BR}(\mu \rightarrow e, \gamma)$, or it will become probed by the next generation of $\mu \rightarrow e, \gamma$ experiments (PSI), scheduled for 2003. For the sake of clarity, we took $\hat{\theta}_1$ real in Fig. 3. The results for $\hat{\theta}_1$ complex are very similar, as can be seen e.g. from eq.(36). Fig. 4 is completely analogous to Fig. 3, but for $\tan \beta = 10$ (instead of $\tan \beta = 3$). It illustrates the strong dependence of $\text{BR}(\mu \rightarrow e, \gamma)$ on $\tan \beta$ in the expected way ($\sim \tan^2 \beta$). An alternative representation of the allowed parameter space is given in Fig.5, where $\hat{\theta}_1$ is given in logarithmic units (the set of supersymmetric parameters corresponds to that of the second plot of Fig.3). These can be more meaningful in particular model-building constructions. Of course, the basic results remain: $\hat{\theta}_1$ should be < 0.12 ($< 3 \times 10^{-3}$) with the present (future) upper bounds on $\text{BR}(\mu \rightarrow e, \gamma)$. This corresponds to $\mathbf{Y}_{31} < 0.04\mathbf{Y}_{33}$ ($\mathbf{Y}_{31} < 9 \times 10^{-4}\mathbf{Y}_{33}$). This gives a measure of the constraints on the textures. (In a logarithmic plot it is not possible to say what percent of the parameter space is allowed since this includes the origin.)

It is worth-noticing from the curves of Figs. 3, 4, the existence of two values of $\hat{\theta}_1$, namely $\hat{\theta}_1 = 0$, $\hat{\theta}_1 \sim 2$, in whose neighborhood the value of $\text{BR}(\mu \rightarrow e, \gamma)$ is drastically suppressed. We will comment shortly on this feature. For large enough values of the universal soft scalar mass, m_0 , $\text{BR}(\mu \rightarrow e, \gamma)$ decreases, as expected: for large m_0 , the branching ratio goes as $\sim m_0^{-4}$, as it is apparent from Fig. 6. Typically, for $\tan \beta = 3$ $\text{BR}(\mu \rightarrow e, \gamma)$ does not fall below the present or forthcoming experimental upper bounds until $m_0 \gtrsim 1.5$ TeV, i.e. beyond the reasonable range to avoid fine-tuning problems. For larger $\tan \beta$, this extremal value increases, since $\text{BR}(\mu \rightarrow e, \gamma) \sim \tan^2 \beta / m_0^4$. Notice that there is a very narrow window at around 120 GeV, for $A_0 = 0$ GeV, where the branching ratio is very suppressed. This happens for every value of $\hat{\theta}_1$ and is the result of a cancellation between the chargino and the neutralino amplitudes.

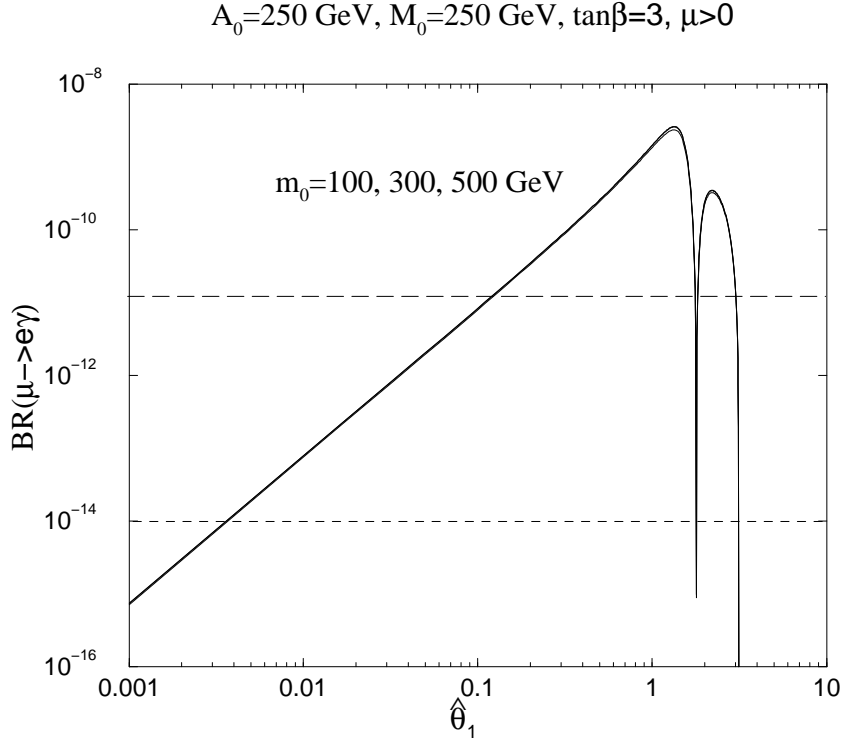


Figure 5: The same as Fig.3 (lower plot) using a logarithmic scale for $\hat{\theta}_1$.

Finally, if one relaxes the unification condition on $|Y_0(M_X)|$, $\text{BR}(\mu \rightarrow e, \gamma)$ logically decreases, as shown in Fig. 7. Anyway, it is noticeable that even for $Y_0(M_X)$ ten times smaller than $Y_t(M_X)$, the conclusion remains that most of the parameter space will be probed in the forthcoming experiments.

4.1.2 Special textures

Let us now turn to the two values of $\hat{\theta}_1$ where $\text{BR}(\mu \rightarrow e, \gamma)$ is suppressed. They correspond to the values for which $(\mathbf{Y}_\nu^+ \mathbf{Y}_\nu)_{21}$, as given by eq.(33), is small. Notice that there are two possible ways to fulfill this requirement, namely $(\mathbf{Y}_\nu)_{31} \simeq 0$ or $(\mathbf{Y}_\nu)_{32} \simeq 0$, which translate into

$$\tan \hat{\theta}_1 \simeq -\sqrt{\frac{\kappa_3}{\kappa_2}} \frac{U_{13}^*}{U_{12}^*} = -\sqrt{\frac{\kappa_3}{\kappa_2}} \frac{V_{13}^*}{V_{12}^*} \simeq 0 \quad (37)$$

$$\tan \hat{\theta}_1 \simeq -\sqrt{\frac{\kappa_3}{\kappa_2}} \frac{U_{23}^*}{U_{22}^*} = -\sqrt{\frac{\kappa_3}{\kappa_2}} \frac{V_{23}^*}{V_{22}^*}, \quad (38)$$

where we have used eqs.(18, 8). We do not know any reason why any of the previous conditions should be satisfied in a particular model, although of course it is not excluded. To this respect, the first condition, i.e. $\hat{\theta}_1 \simeq 0$, seems to be more “natural”

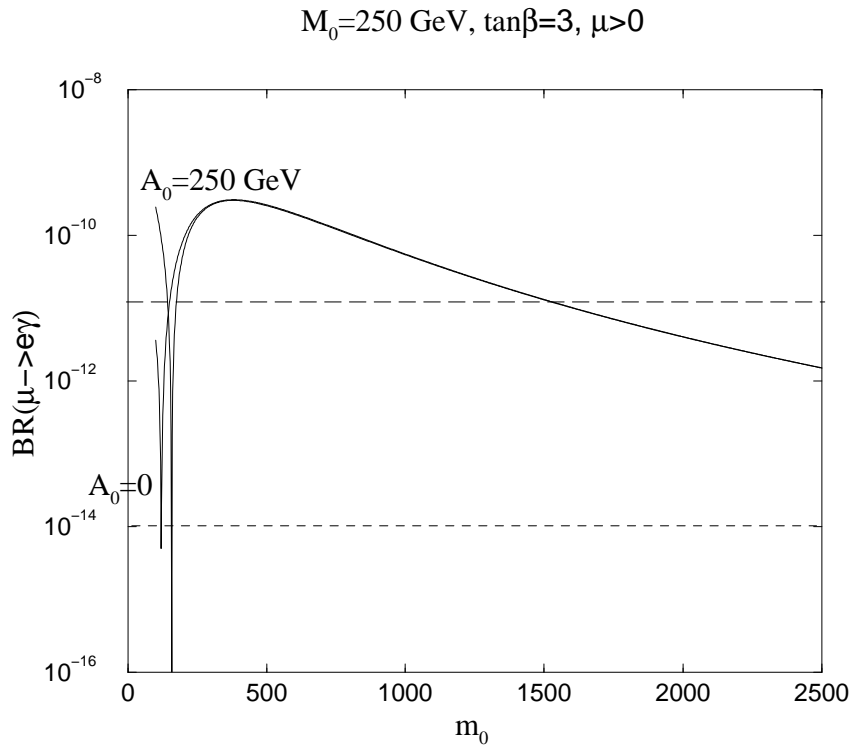


Figure 6: Branching ratio of the process $\mu \rightarrow e, \gamma$ vs. the universal scalar mass, m_0 , in the case of hierarchical (left and right) neutrinos, and for the two sets of supersymmetric parameters of Fig. 3 (with $\tan\beta = 3$) and $\hat{\theta}_1 = 0.5$. The dashed lines correspond to the present and forthcoming upper bounds. Except for a narrow range at low energy, the prediction does not fall below the present upper bound until $m_0 > 1.5 \text{ TeV}$. The same occurs for other values of $\hat{\theta}_1$, except for the two special values seeable in Fig. 3 and discussed in subsect. 4.1.2.

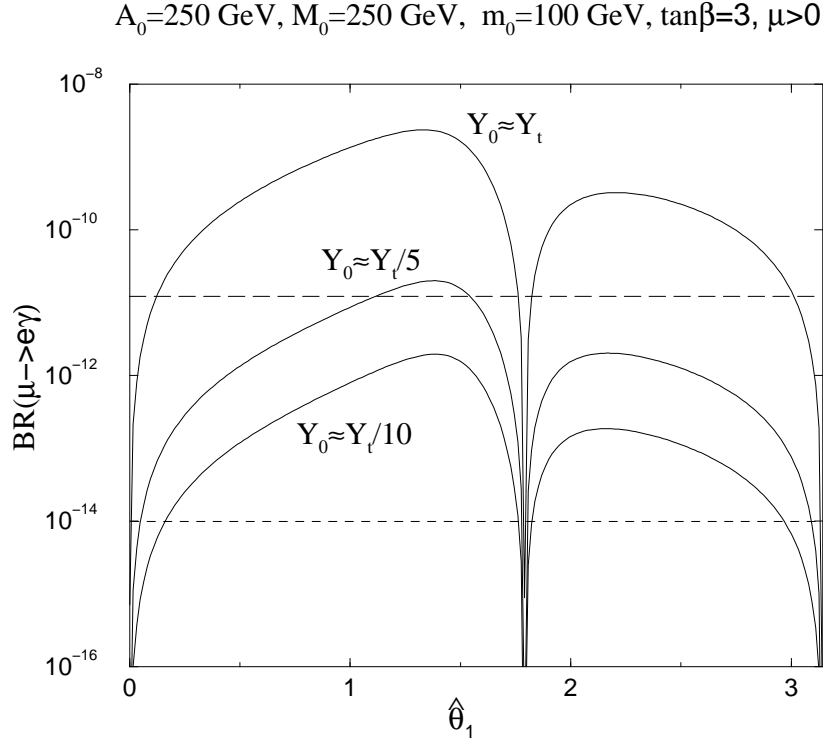


Figure 7: The same as Fig. 3 (lower plot) for different values of the largest neutrino Yukawa coupling, Y_0 , at the “unification” scale, M_X . Y_t denotes the value of the top Yukawa coupling at that scale.

to obtain than the second one: note that $\hat{\theta}_i = 0$, i.e. $R = \mathbf{1}$, corresponds to the case where all the mixing can be attributed to the sector of charged leptons, as discussed in sect. 2, which is a physical possibility. It is interesting to explicitly show the textures of \mathbf{Y}_ν that correspond to these ‘privileged’ values of $\hat{\theta}_1$ from eqs.(37, 38). They read, respectively,

$$\mathbf{Y}_\nu \propto \begin{pmatrix} 0 & 0 & 0 \\ 0 & 0 & 0 \\ 0 & V_{31} & -V_{21} \end{pmatrix} \propto \begin{pmatrix} 0 & 0 & 0 \\ 0 & 0 & 0 \\ 0 & 1 & 1 \end{pmatrix}, \quad (39)$$

$$\mathbf{Y}_\nu \propto \begin{pmatrix} 0 & 0 & 0 \\ 0 & 0 & 0 \\ -V_{31} & 0 & V_{11} \end{pmatrix} \propto \begin{pmatrix} 0 & 0 & 0 \\ 0 & 0 & 0 \\ -1 & 0 & \sqrt{2} \end{pmatrix}. \quad (40)$$

Here we have used $\text{Im}V_{11} = 0$ and $s_{13} \ll 1$, so that $\text{Im}V_{21}, \text{Im}V_{31} \ll 1$. Besides, the numerical values of the entries in (39, 40) correspond to a bimaximal mixing V matrix, which includes the preferred LAMSW scenario. Let us stress that the previous textures are to be understood in the basis we have chosen to work, i.e. where both \mathbf{Y}_e and \mathcal{M} are diagonal, and the latter has the eigenvalues ordered in the usual hierarchical way shown in eq.(32). It is interesting to note that texture (39) has been advocated in

ref.[27] on different grounds.

Some comments are in order here. As was discussed in subsect. 2.1, the first two rows of \mathbf{Y}_ν , though suppressed, are normally important to reconstruct κ from \mathbf{Y}_ν , \mathcal{M} . In particular, for texture (40) the precise values of the first two rows are crucial to reproduce the bimaximal structure of κ . On the other hand, this is not necessarily the case for texture (39). Actually, it is remarkable that texture (39) works fine, both to reproduce κ and to give suppressed $\text{BR}(\mu \rightarrow e, \gamma)$, even if it is given in a basis where \mathcal{M} is not diagonal.

In general, it is clear from eq.(33) that the $l_i \rightarrow l_j, \gamma$ process is suppressed at the points in the parameter space where $(\mathbf{Y}_\nu)_{3i} \simeq 0$ or $(\mathbf{Y}_\nu)_{3j} \simeq 0$. Therefore, there are three special textures: the two given in the above eqs.(39, 40), which correspond to $(\mathbf{Y}_\nu)_{31} \simeq 0$ and $(\mathbf{Y}_\nu)_{32} \simeq 0$, and the one corresponding to $(\mathbf{Y}_\nu)_{33} \simeq 0$. The latter implies

$$\tan \hat{\theta}_1 \simeq -\sqrt{\frac{\kappa_3}{\kappa_2}} \frac{U_{33}^*}{U_{32}^*} = -\sqrt{\frac{\kappa_3}{\kappa_2}} \frac{V_{33}^*}{V_{32}^*} , \quad (41)$$

and the associated texture is

$$\mathbf{Y}_\nu \propto \begin{pmatrix} 0 & 0 & 0 \\ 0 & 0 & 0 \\ V_{21} & -V_{11} & 0 \end{pmatrix} \propto \begin{pmatrix} 0 & 0 & 0 \\ 0 & 0 & 0 \\ -1 & \sqrt{2} & 0 \end{pmatrix} , \quad (42)$$

where, again, the numerical values correspond to the bimaximal scenario. If the texture of \mathbf{Y}_ν is one of the special forms (39, 40, 42), there are two $l_i \rightarrow l_j, \gamma$ processes suppressed and one unsuppressed. This means that for those privileged cases where $\mu \rightarrow e, \gamma$ is unusually suppressed, the $\tau \rightarrow \mu, \gamma$ and $\tau \rightarrow e, \gamma$ processes are relevant and may give the most important restrictions on models. In particular, if \mathbf{Y}_ν is as in eq.(39) or eq.(40) (i.e. $(\mathbf{Y}_\nu)_{31} \simeq 0$ or $(\mathbf{Y}_\nu)_{32} \simeq 0$), then $\text{BR}(\tau \rightarrow \mu, \gamma)$ or $\text{BR}(\tau \rightarrow e, \gamma)$ respectively are unsuppressed.

We have illustrated this interesting aspect by plotting $\text{BR}(\tau \rightarrow \mu, \gamma)$ vs. $\hat{\theta}_1$ in Fig. 8 for one of the typical supersymmetric scenarios considered in Fig. 3. Notice that for the special value $\hat{\theta}_1 \simeq 0$, at which $\text{BR}(\mu \rightarrow e, \gamma)$ is suppressed, $\text{BR}(\tau \rightarrow \mu, \gamma)$ is not, lying above the forthcoming experimental upper bound.

4.1.3 The contribution $\propto \mathcal{M}_2$

So far, all the results of this subsection have been obtained neglecting the value of \mathcal{M}_2 (see eq.(32)). Let us consider here a value of $\mathcal{M}_2 \neq 0$, though smaller than \mathcal{M}_3 , as it

$A_0=250 \text{ GeV}, M_0=250 \text{ GeV}, \tan\beta=3, \mu>0$

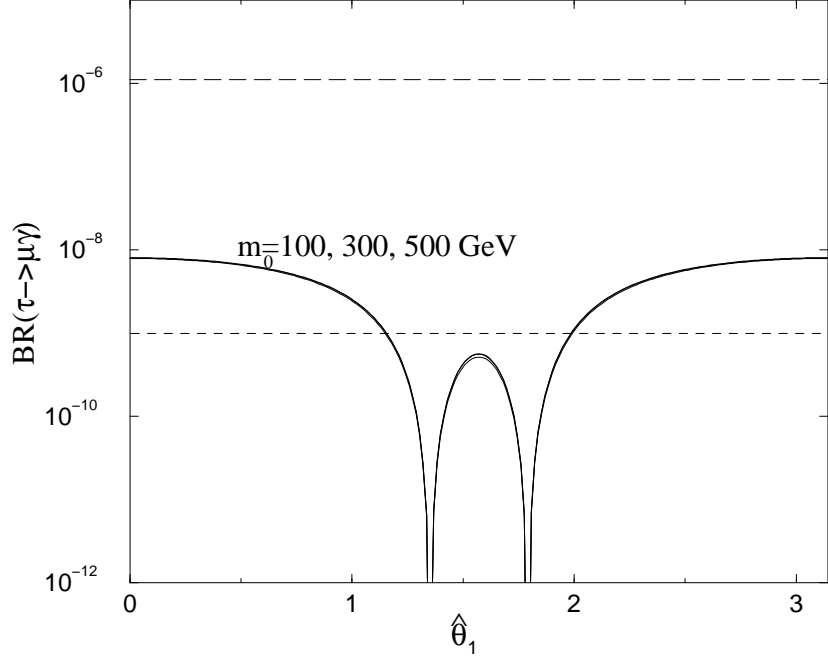


Figure 8: The same as Fig. 3 (lower plot), but for the branching ratio of the process $\tau \rightarrow \mu, \gamma$. The dashed lines correspond to the present and forthcoming upper bounds.

was done in ref.[10].

Clearly, for generic values $\hat{\theta}_i$, the contributions already computed [see eqs.(34–36)] will be the dominant ones. However, if $\hat{\theta}_1$ corresponds to one of the particular values of eqs.(37, 38), the contributions $\sim \mathcal{M}_2$ can be relevant or even dominant. Normally, this will happen only for $\hat{\theta}_1$ quite close to eqs.(37, 38). Suppose for example that $R \simeq \mathbf{1}$, i.e. \hat{s}_i small and real. This corresponds to eq.(37) and it is probably the most interesting case (and the one considered in ref. [10]). Then $(\mathbf{Y}_\nu^+ \mathbf{Y}_\nu)_{ij} = (\mathbf{Y}_\nu)_{2i}^* (\mathbf{Y}_\nu)_{2j} + (\mathbf{Y}_\nu)_{3i}^* (\mathbf{Y}_\nu)_{3j}$ with \mathbf{Y}_ν given by eq.(13). Keeping only terms up to $\mathcal{O}(\hat{s}_i)$ we get

$$\begin{aligned}
 (\mathbf{Y}_\nu^+ \mathbf{Y}_\nu)_{21} &\simeq \mathcal{M}_2 \kappa_2 U_{12}^* U_{22} + \mathcal{M}_3 \kappa_3 U_{13}^* U_{23} \\
 &+ \hat{s}_1 (\mathcal{M}_3 - \mathcal{M}_2) \sqrt{\kappa_2 \kappa_3} (U_{13}^* U_{22} + U_{12}^* U_{23}), \quad (43)
 \end{aligned}$$

so that in a bimaximal case, even taking $U_{13} = 0$, the part proportional to \mathcal{M}_3 will be indeed the dominant one except for $\hat{s}_1 \lesssim (\mathcal{M}_2/\mathcal{M}_3) (\sqrt{\kappa_2/\kappa_3})$, i.e. very close to zero.

For the specific case $R = \mathbf{1}$, i.e. $\hat{s}_1 = 0$, we get $(\mathbf{Y}_\nu^+ \mathbf{Y}_\nu)_{21} \simeq \mathcal{M}_2 \kappa_2 U_{12}^* U_{22}$. Taking into account from eq.(35) $|Y_0|^2 = \mathcal{M}_3 \kappa_3$, the value of $(\mathbf{Y}_\nu^+ \mathbf{Y}_\nu)_{21}$ is exactly as the one

we will obtain in another context in subsect. 4.2, see eq.(48) below, but multiplied by $\mathcal{M}_2/\mathcal{M}_3$. In consequence, the plots of $\text{BR}(\mu \rightarrow e, \gamma)$ are identical to those of Fig. 9 below, but multiplied by $(\mathcal{M}_2/\mathcal{M}_3)^2$. For $\mathcal{M}_2/\mathcal{M}_3 \gtrsim 10^{-2}$ the branching ratio is still testable in the forthcoming generation of experiments.

4.1.4 $R_{32} \simeq R_{33} \simeq 0$

So far we have assumed $R_{32} \neq 0$ or $R_{33} \neq 0$ in eq.(13). Recall that R is an unknown orthogonal matrix. The experimental data do not restrict its form, although R may be much more definite in specific models. We consider now the special case when $R_{32} \simeq R_{33} \simeq 0$. It should be kept in mind that this represents a narrow region of the whole parameter space of R .

However, as we are about to see, this possibility includes the particular case where all the leptonic flavour violation can be attributed to the sector of right-handed neutrinos. This happens when there exists a basis in which \mathbf{Y}_e and \mathbf{Y}_ν get simultaneously diagonal, while \mathcal{M} gets non-diagonal. This is physically interesting and it can occur in particular models. As explained in sect. 2, in the basis we have chosen to work (\mathbf{Y}_e and \mathcal{M} diagonal), this implies $\mathbf{Y}_\nu = W D_Y$, where D_Y is a diagonal matrix and W is a unitary matrix. Hence, $\mathbf{Y}_\nu^\dagger \mathbf{Y}_\nu = D_{|Y^2|}$. Then, from the general equation (13) or (14), we get

$$R^\dagger D_{\mathcal{M}} R = D_{\sqrt{\kappa-1}} U^\dagger D_{|Y^2|} U D_{\sqrt{\kappa-1}} . \quad (44)$$

If U is of the bimaximal type, as it occurs in the preferred LAMSW scenario, then $U_{i1} \neq 0$ for any i [see eq.(31)]. This means that, in first approximation, the only non-vanishing entry of the right hand side of eq.(44) is the (1,1), so the same holds for the left hand side. Since $D_{\mathcal{M}}$ is hierarchical, $(R^\dagger D_{\mathcal{M}} R)_{ij} \simeq R_{3i}^* \mathcal{M}_3 R_{3j}$. Thus, $R_{32} \simeq R_{33} \simeq 0$ *q.e.d.* A special case occurs when $D_{|Y^2|} = |Y_0^2| \mathbf{1}$. Then eq.(44) becomes $R^\dagger D_{\mathcal{M}} R = |Y_0^2| D_{\kappa-1}$ for any form of U ; and R turns out to be simply the ‘‘permutation matrix’’ that interchanges the 1- and 3-planes: $R = R_p = \{(0, 0, \pm 1), (0, \pm 1, 0), (\pm 1, 0, 0)\}$. Of course, in all these cases, since $\mathbf{Y}_\nu^\dagger \mathbf{Y}_\nu$ is diagonal, there is no RG generation of non-diagonal soft terms, and the predictions for $\text{BR}(l_i \rightarrow l_j, \gamma)$ are as in the SM, i.e. negligible.

Nevertheless, the possibility $R_{32} \simeq R_{33} \simeq 0$ includes other cases different than the previous (almost trivial) one. As mentioned, this represents a small region of the

parameter space, which in principle has no special physical significance; but for the sake of completeness we will analyze it. R will admit the parametrization

$$R \simeq \begin{pmatrix} 0 & \pm\hat{c} & \hat{s} \\ 0 & \mp\hat{s} & \hat{c} \\ \pm 1 & 0 & 0 \end{pmatrix}, \quad (45)$$

where $\hat{\theta}$ is an arbitrary complex angle and the sign of the ± 1 entry is not correlated to the signs appearing in the second column. Thus, from eq.(13), and keeping only the dominant terms,

$$\mathbf{Y}_\nu \simeq \begin{pmatrix} 0 & \pm\sqrt{\mathcal{M}_1\hat{c}\sqrt{\kappa_2}} & \sqrt{\mathcal{M}_1\hat{s}\sqrt{\kappa_3}} \\ 0 & \mp\sqrt{\mathcal{M}_2\hat{s}\sqrt{\kappa_2}} & \sqrt{\mathcal{M}_2\hat{c}\sqrt{\kappa_3}} \\ \pm\sqrt{\mathcal{M}_3\kappa_1} & 0 & 0 \end{pmatrix} U^+, \quad (46)$$

Therefore, the values of $(\mathbf{Y}_\nu^+\mathbf{Y}_\nu)_{ij}$, $i \neq j$, which are the relevant quantities for $l_i \rightarrow l_j, \gamma$, depend on the value of \hat{s} . In general, if a unification condition is imposed for the largest eigenvalue of $\mathbf{Y}_\nu^+\mathbf{Y}_\nu$, then $(\mathbf{Y}_\nu^+\mathbf{Y}_\nu)_{21}$ is quite large and $\text{BR}(\mu \rightarrow e, \gamma)$ is above the experimental limit.

Let us illustrate the last point with an example: suppose that $\hat{s} = \pm 1$ in eq.(46). Then the eigenvalues of $\mathbf{Y}_\nu^+\mathbf{Y}_\nu$ are $\{\mathcal{M}_3\kappa_1, \mathcal{M}_2\kappa_2, \mathcal{M}_1\kappa_3\}$. If they are degenerate, $\mathbf{Y}_\nu^+\mathbf{Y}_\nu$ is diagonal and we are in the above-considered case: all the mixing can be attributed to the sector of right-handed neutrinos. If not, since $U_{13} \simeq 0$, then $(\mathbf{Y}_\nu^+\mathbf{Y}_\nu)_{21} \simeq U_{11}^*U_{21}\mathcal{M}_3\kappa_1 + U_{12}^*U_{22}\mathcal{M}_2\kappa_2$. This is at least as large as the matrix element computed in the generic case, eq.(36), thus leading to unacceptably large $\text{BR}(\mu \rightarrow e, \gamma)$. For generic values of \hat{s} the analysis is more involved, but at the end of the day the conclusion is similar.

4.2 ν_L 's hierarchical and ν_R 's degenerate

As was discussed in subsect. 2.2, if the R matrix is real, this scenario is extremely predictive. In particular $\mathbf{Y}_\nu^+\mathbf{Y}_\nu$ is given by eq.(21), which does not depend on the form of R . More precisely

$$(\mathbf{Y}_\nu^+\mathbf{Y}_\nu)_{ij} = \mathcal{M}\kappa_i U_{il} U_{lj}^+ \simeq \mathcal{M} [\kappa_2 U_{i2} U_{j2}^* + \kappa_3 U_{i3} U_{j3}^*], \quad (47)$$

where $\kappa_2 \equiv \kappa_{sol}$ and $\kappa_3 \equiv \kappa_{atm}$. The free parameter \mathcal{M} can be absorbed in the value of the largest eigenvalue of the $\mathbf{Y}_\nu^+\mathbf{Y}_\nu$ matrix, $|Y_0|^2 \simeq \mathcal{M}\kappa_3$. In particular, the matrix

element $(\mathbf{Y}_\nu^+ \mathbf{Y}_\nu)_{21}$ becomes

$$(\mathbf{Y}_\nu^+ \mathbf{Y}_\nu)_{21} \simeq \mathcal{M} \kappa_2 U_{22} U_{12}^* = |Y_0|^2 \frac{\kappa_2}{\kappa_3} U_{22} U_{12}^* , \quad (48)$$

where we have used $U_{13} \simeq 0$. Comparing (48) with (36), we see that in this scenario we expect predictions for $\text{BR}(\mu \rightarrow e, \gamma)$ and the other processes of the same order as for hierarchical neutrinos (more precisely, $\sim \kappa_2/\kappa_3$ times smaller), but with no special textures where the branching ratio becomes suppressed. All this is illustrated in Fig. 9. for the LAMSW scenario using $|Y_0(M_X)| = |Y_t(M_X)|$.

From the plots, it is clear that in this scenario $\text{BR}(\mu \rightarrow e, \gamma)$ is already above the present experimental limits except for a rather small region of m_0 -values which should be probed by the next generation of experiments.

If R is complex, the analysis is more involved since it contains more arbitrary parameters; but in general the conclusion is the same: $\text{BR}(\mu \rightarrow e, \gamma)$ is at least of the same order as in the real case. To see this note that from the general equation (14)

$$\begin{aligned} (\mathbf{Y}_\nu^+ \mathbf{Y}_\nu)_{21} &= \mathcal{M} \left[U_{2p} \sqrt{\kappa_p} (R^+ R)_{pq} \sqrt{\kappa_q} U_{1q}^* \right] \\ &\simeq \mathcal{M} \left[U_{23} U_{12}^* \sqrt{\kappa_3 \kappa_2} R_{q3}^* R_{q2} + U_{22} U_{12}^* \kappa_2 R_{q2}^* R_{q2} \right] . \end{aligned} \quad (49)$$

Normally, this is at least of the same order as in the real case, eq.(48), as we have checked numerically. Now there exists, however, the possibility of a (fine-tuned) cancellation between the various contributions of (49). In particular such cancellation will occur if all the mixing can be attributed to the sector of right-handed neutrinos, which implies $\mathbf{Y}_\nu^+ \mathbf{Y}_\nu$ diagonal.

4.3 ν_L 's quasi-degenerate

As it was discussed in subsect. 2.3, in this case it is logical to assume that \mathcal{M} has degenerate eigenvalues. If, furthermore, the R matrix is real, we get from eq.(14)

$$\mathbf{Y}_\nu^+ \mathbf{Y}_\nu = \mathcal{M} U D_\kappa U^+ , \quad (50)$$

Incidentally, for R real the requirement that for quasi-degenerate neutrinos the two CP phases, ϕ and ϕ' , are opposite in order to be consistent with ν -less double β decay [28], implies that U and thus \mathbf{Y}_ν is complex, see eqs.(8, 9, 13).

Since $\kappa_1 \simeq \kappa_2 \simeq \kappa_3 \equiv \kappa$ (typically $\kappa = \mathcal{O}(1\text{eV}/v_2^2)$), the eigenvalues of $\mathbf{Y}_\nu^+ \mathbf{Y}_\nu$ are quasi-degenerate $\sim \mathcal{M} \kappa \equiv |Y_0|^2$. Clearly, eq.(50) presents a GIM-like suppression,

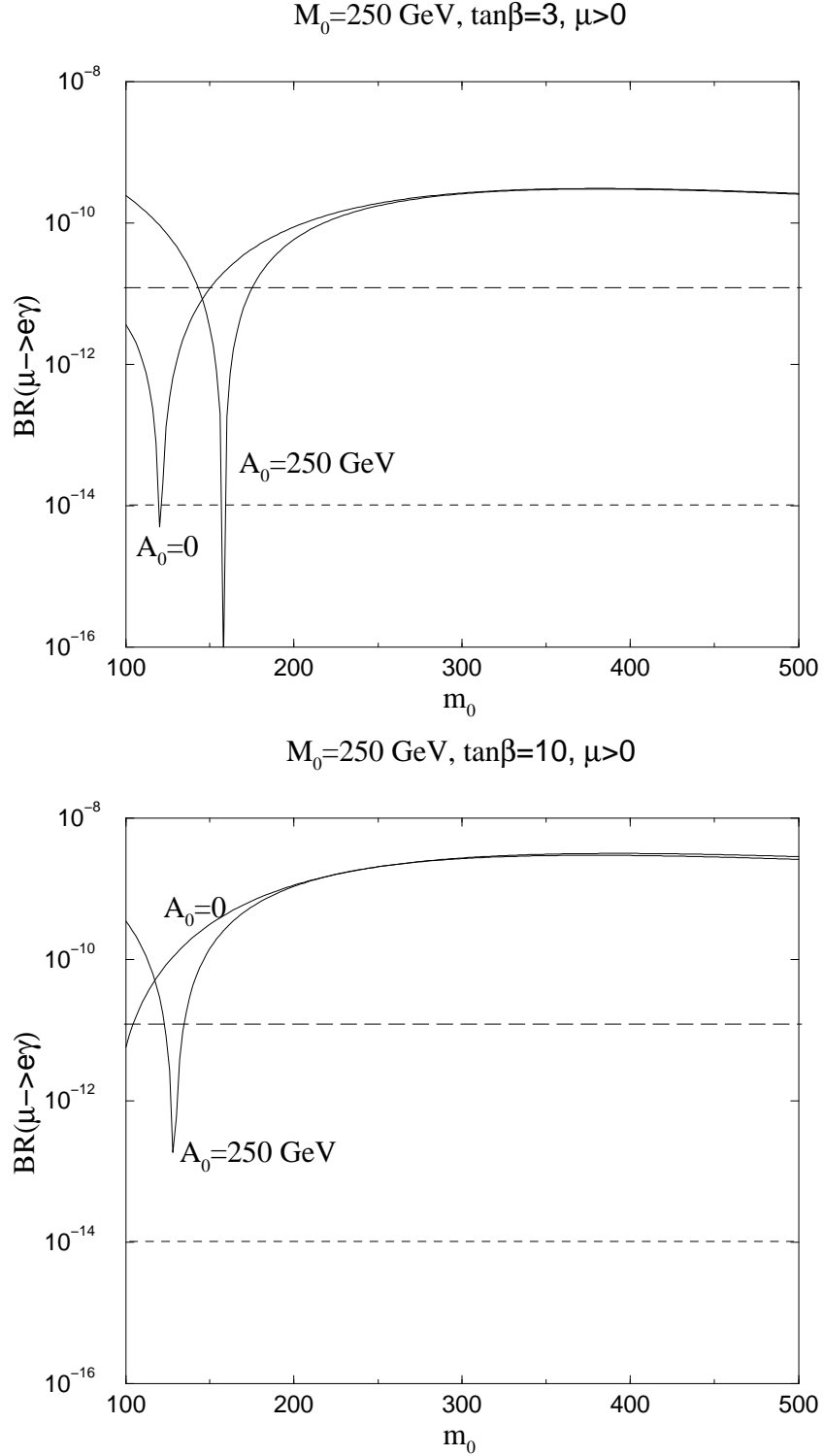


Figure 9: Branching ratio of the process $\mu \rightarrow e, \gamma$ vs. the universal scalar mass, m_0 , for the case of hierarchical (degenerate) left (right) neutrinos, R real (see subsect. 4.2) and two typical sets of supersymmetric parameters, as indicated in the plots. The dashed lines correspond to the present and forthcoming upper bounds. A top-neutrino “unification” condition has been used to fix the value of the largest neutrino Yukawa coupling at high energy. The two plots illustrate two different values of $\tan\beta$. The curves do not fall below the present bound until $m_0 > 1.6 \text{ TeV}$ (upper plot) and $m_0 > 2.9 \text{ TeV}$ (lower plot).

so the off-diagonal entries of $\mathbf{Y}_\nu^+ \mathbf{Y}_\nu$ are small and proportional to the differences of neutrinos masses. More precisely, for $i \neq j$

$$(\mathbf{Y}_\nu^+ \mathbf{Y}_\nu)_{ij} = \mathcal{M} U_{ip} U_{jp}^* \kappa_p = \mathcal{M} U_{ip} U_{jp}^* (\kappa_p - \kappa_3) \quad . \quad (51)$$

In particular, the matrix element $(\mathbf{Y}_\nu^+ \mathbf{Y}_\nu)_{21}$, which is the relevant one for $\mu \rightarrow e, \gamma$, becomes

$$(\mathbf{Y}_\nu^+ \mathbf{Y}_\nu)_{21} = \mathcal{M} [U_{21} U_{11}^* (\kappa_1 - \kappa_3) + U_{22} U_{12}^* (\kappa_2 - \kappa_3)] \quad . \quad (52)$$

Since $U_{13} \simeq 0$,⁶ from unitarity follows that $U_{21} U_{11}^* \simeq -U_{22} U_{12}^*$. So

$$(\mathbf{Y}_\nu^+ \mathbf{Y}_\nu)_{21} = \mathcal{M} [U_{21} U_{11}^* (\kappa_1 - \kappa_2)] = |Y_0|^2 U_{21} U_{11} \frac{\Delta \kappa_{sol}^2}{\kappa^2} \quad . \quad (53)$$

The factor $\frac{\Delta \kappa_{sol}^2}{\kappa^2}$ is at most $\sim 10^{-5}$ (this occurs for the LAMSW solution to the solar neutrino problem), which implies a drastic suppression of $(\mathbf{Y}_\nu^+ \mathbf{Y}_\nu)_{21}$, and thus of $\text{BR}(\mu \rightarrow e, \gamma)$ in this kind of scenario. More quantitatively, eq.(53) is identical to eq.(48) (i.e. the scenario where ν_L 's are hierarchical and ν_R 's degenerate), multiplied by $\kappa^{-2} \sqrt{\Delta \kappa_{sol}^2 \Delta \kappa_{atm}^2}$. This is a factor $\sim 10^{-4}$ for the LAMSW, which means that all the plots representing $\text{BR}(\mu \rightarrow e, \gamma)$ in that scenario (Fig. 9) are identical here, but with the vertical axis re-scaled eight orders of magnitude smaller.

If the R matrix is complex, then $R^+ R$ is in general non-diagonal, so the $\mathbf{Y}_\nu^+ \mathbf{Y}_\nu$ matrix becomes

$$\mathbf{Y}_\nu^+ \mathbf{Y}_\nu = \mathcal{M} U D_{\sqrt{\kappa}} R^+ R D_{\sqrt{\kappa}} U^+ \quad , \quad (54)$$

which may have sizeable off-diagonal entries. Hence, even for quasi-degenerate neutrinos, $(\mathbf{Y}_\nu^+ \mathbf{Y}_\nu)_{21}$, and thus $\text{BR}(\mu \rightarrow e, \gamma)$, could be very large if R is complex.

Finally, we would like to comment on the scenario where the neutrinos are partially degenerate, i.e. when their masses present an inverse hierarchy: $\kappa_3 \ll \kappa_1 \simeq \kappa_2 \equiv \kappa$. [It is convenient to maintain κ_3 as the most split mass eigenvalue, so that the interpretation of θ_{23}, θ_{12} as the atmospheric and solar angles respectively remains valid.] Notice that in this case $\kappa^2 \simeq \Delta \kappa_{atm}^2$.

⁶Since we are working here with quasi-degenerate neutrinos, one may wonder whether the low-energy condition $U_{13} \simeq 0$ might change at the \mathcal{M} scale. However, as it was shown in ref.[29], the U_{13} element is stable under the RG running between \mathcal{M} and low-energy for any phenomenologically viable scenario. Therefore, the argument that follows is completely general.

Now, the discussion of the size of $(\mathbf{Y}_\nu^+ \mathbf{Y}_\nu)_{21}$, and thus of $\text{BR}(\mu \rightarrow e, \gamma)$, is similar to that in the complete degenerate case, though the conclusions are different. In particular, suppose that \mathcal{M} has degenerate eigenvalues, $D_{\mathcal{M}} = \text{diag}(\mathcal{M}, \mathcal{M}, \mathcal{M})$, and that the R matrix is real. Then eq.(50) holds, so $\mathbf{Y}_\nu^+ \mathbf{Y}_\nu$ has two large quasi-degenerate eigenvalues $\sim \mathcal{M}\kappa \equiv |Y_0|^2$. Likewise, all the discussion between the eqs. (51)–(53) and the equations themselves remain valid. Therefore, the matrix element $(\mathbf{Y}_\nu^+ \mathbf{Y}_\nu)_{21}$ becomes

$$(\mathbf{Y}_\nu^+ \mathbf{Y}_\nu)_{21} = |Y_0|^2 U_{21} U_{11}^* \frac{\Delta\kappa_{sol}^2}{\kappa^2} = |Y_0|^2 U_{21} U_{11}^* \frac{\Delta\kappa_{sol}^2}{\Delta\kappa_{atm}^2} . \quad (55)$$

Again, this equation is identical to eq.(48), multiplied now by $\sqrt{\frac{\Delta\kappa_{sol}^2}{\Delta\kappa_{atm}^2}}$. This suppression factor is not as strong as before. Namely, it is $\sim 10^{-1}$ for the LAMSW, which means that all the plots representing $\text{BR}(\mu \rightarrow e, \gamma)$ in this scenario are as in the one where ν_L 's are hierarchical and ν_R 's degenerate, re-scaled by a factor $\sim 10^{-2}$. Hence, from Fig. 9 it is clear that $\text{BR}(\mu \rightarrow e, \gamma)$ for the partially degenerate case should be testable within the next generation of experiments.

The matrix element $(\mathbf{Y}_\nu^+ \mathbf{Y}_\nu)_{31}$ gets a similar suppression. However $(\mathbf{Y}_\nu^+ \mathbf{Y}_\nu)_{32}$ is not suppressed at all:

$$(\mathbf{Y}_\nu^+ \mathbf{Y}_\nu)_{32} = \mathcal{M} [U_{31} U_{21}^* (\kappa_1 - \kappa_3) + U_{32} U_{22}^* (\kappa_2 - \kappa_3)] \simeq \mathcal{M}\kappa [U_{31} U_{21}^* + U_{32} U_{22}^*] , \quad (56)$$

where $\mathcal{M}\kappa = |Y_0|^2$. This is a similar size to that from the hierarchical scenarios. So, for the partially degenerate case, $\text{BR}(\tau \rightarrow \mu, \gamma)$ should also be testable in the next generation of experiments.

Again, if the R matrix is complex $\mathbf{Y}_\nu^+ \mathbf{Y}_\nu$ is given by eq.(54) and we expect much larger values for $(\mathbf{Y}_\nu^+ \mathbf{Y}_\nu)_{21}$, $(\mathbf{Y}_\nu^+ \mathbf{Y}_\nu)_{31}$.

5 Summary of predictions for $\text{BR}(l_i \rightarrow l_j, \gamma)$

If the origin of the neutrino masses is a see-saw mechanism, implemented in a supersymmetric theory, the soft breaking terms get off-diagonal contributions through the RG running, even if one starts with a universality condition for the soft terms. E.g. for the slepton doublet mass-matrix, at the leading-log approximation,

$$(m_L^2)_{ij} \simeq \frac{-1}{8\pi^2} (3m_0^2 + A_0^2) (\mathbf{Y}_\nu^+ \mathbf{Y}_\nu)_{ij} \log \frac{M_X}{M} , \quad (57)$$

where \mathbf{Y}_ν is the matrix of neutrino Yukawa couplings, M is the typical (Majorana) mass of the right-handed neutrinos and M_X is the initial scale at which universality is imposed. Therefore, the predictions on $\text{BR}(l_i \rightarrow l_j, \gamma)$ are directly linked to the size of $(\mathbf{Y}_\nu^\dagger \mathbf{Y}_\nu)_{ij}$. Moreover, the larger (smaller) the initial scale at which universality is imposed the larger the branching ratios. Also, due to the structure of the diagrams, $\text{BR}(l_i \rightarrow l_j, \gamma)$ has a strong dependence on $\tan\beta$ ($\sim \tan^2\beta$). The most general form of \mathbf{Y}_ν and thus of $\mathbf{Y}_\nu^\dagger \mathbf{Y}_\nu$, in terms of measurable low-energy parameters has been determined in sect. 2. In particular, working in the flavour basis in which the gauge interactions and the charged-lepton Yukawa matrix, \mathbf{Y}_e , are flavour-diagonal,

$$\mathbf{Y}_\nu^\dagger \mathbf{Y}_\nu = U D_{\sqrt{\kappa}} R^\dagger D_{\mathcal{M}} R D_{\sqrt{\kappa}} U^\dagger \quad (58)$$

Here $D_{\sqrt{\kappa}}$ is the diagonal matrix of positive neutrino mass eigenvalues ($\kappa = \mathcal{M}_\nu / \langle H_2^0 \rangle^2$), while U contains the mixing angles and CP phases [see eqs.(6, 7)]. In addition, $\mathbf{Y}_\nu^\dagger \mathbf{Y}_\nu$ depends on unknown parameters: the three positive mass eigenvalues of the righthanded neutrinos (contained in $D_{\mathcal{M}}$) and the three complex parameters defining the complex orthogonal matrix R . In practical cases, however, the number of relevant free parameters becomes drastically reduced.

Next, we enumerate the possible low-energy scenarios and the corresponding predictions for $(\mathbf{Y}_\nu^\dagger \mathbf{Y}_\nu)_{ij}$ and $\text{BR}(l_i \rightarrow l_j, \gamma)$, as has been worked out in detail in sects. 2, 3, 4.

ν_L 's and ν_R 's completely hierarchical

- If R is a generic matrix, $(\mathbf{Y}_\nu^\dagger \mathbf{Y}_\nu)_{ij}$ is given by eq.(33). Using the parametrization of R given in eq.(17), which is sufficiently general for this case, one obtains in particular

$$(\mathbf{Y}_\nu^\dagger \mathbf{Y}_\nu)_{21} \sim \frac{|Y_0|^2}{|\hat{s}_1|^2 \kappa_2 + |\hat{c}_1|^2 \kappa_3} \hat{c}_1^* \hat{s}_1 \sqrt{\kappa_3 \kappa_2} U_{23} U_{12}^* \quad (59)$$

Here $|Y_0|^2$ is the largest eigenvalue of $\mathbf{Y}_\nu^\dagger \mathbf{Y}_\nu$ [see eq.(35)] and $\hat{\theta}_1$ is an arbitrary complex angle.

For the LAMSW scenario the previous equation generically gives $\text{BR}(\mu \rightarrow e, \gamma)$ above the *present* experimental limits, at least for $Y_0 = \mathcal{O}(1)$, as it occurs in the unified scenarios. This is illustrated in Figs. 3, 4, 5, 6 using $|Y_0(M_X)| = |Y_t(M_X)|$,

with $M_X = 2 \times 10^{16}$ GeV. But even for $Y_0 = \mathcal{O}(10^{-1})$, most of the parameter space will be probed in the forthcoming generation of experiments experiments (see Fig. 7).

- The only exceptions to the previous result are
 - If $\hat{\theta}_1$ takes one of the two values given in eqs.(37, 38), which correspond to the textures of eqs.(39, 40). Then, $\text{BR}(\mu \rightarrow e, \gamma)$ is drastically reduced, but other processes, as $\text{BR}(\tau \rightarrow \mu, \gamma)$, are not, normally lying above the forthcoming experimental upper bound, see Fig. 8.
 - If R is such that $\mathbf{Y}_\nu^+ \mathbf{Y}_\nu$ is diagonal. This means that in a certain basis \mathbf{Y}_e and \mathbf{Y}_ν are diagonal whereas the right-handed Majorana mass matrix, \mathcal{M} , is not. This requires a very special form of R , which in particular has $R_{32}, R_{33} \simeq 0$. Of course, in this special case there is no RG generation of non-diagonal soft terms, and the predictions for $\text{BR}(l_i \rightarrow l_j, \gamma)$ are as in the SM, i.e. negligible.

ν_L 's hierarchical and ν_R 's degenerate

- If R is real, this scenario is very predictive. $(\mathbf{Y}_\nu^+ \mathbf{Y}_\nu)_{ij}$ is given by eq.(47). In particular, taking into account $U_{13} \simeq 0$,

$$(\mathbf{Y}_\nu^+ \mathbf{Y}_\nu)_{21} \simeq \mathcal{M} \kappa_2 U_{22} U_{12}^* = |Y_0|^2 \frac{\kappa_2}{\kappa_3} U_{22} U_{12}^* , \quad (60)$$

where $|Y_0|^2 \simeq \mathcal{M} \kappa_3$ is the largest eigenvalue of $\mathbf{Y}_\nu^+ \mathbf{Y}_\nu$.

The corresponding $\text{BR}(\mu \rightarrow e, \gamma)$ is shown in Fig. 9. for the LAMSW scenario, and using $|Y_0(M_X)| = |Y_t(M_X)|$.⁷ The branching ratio turns out to be already above the present experimental limits except for a rather small region of m_0 values which should be probed by the next generation of experiments. Here are not special textures where the branching ratio becomes suppressed.

- If R is complex, the analysis is more involved since it contains more arbitrary parameters; $(\mathbf{Y}_\nu^+ \mathbf{Y}_\nu)_{21}$ is given by eq.(49). But in general the conclusion is the same: $\text{BR}(\mu \rightarrow e, \gamma)$ is at least of the same order as in the real case. Now there

⁷For other values of $|Y_0|$ note that $\text{BR}(\mu \rightarrow e, \gamma) \sim |Y_0|^4$. Actually, this dependence is milder, since the larger $|Y_0(M_X)|$, the faster it decreases with the scale.

exists, however, the possibility of a (fine-tuned) cancellation between the various contributions of (49). In particular such cancellation will occur if all the mixing can be attributed to the sector of right-handed neutrinos, which implies $\mathbf{Y}_\nu^+\mathbf{Y}_\nu$ diagonal.

ν_L 's quasi-degenerate

- If R is real, $(\mathbf{Y}_\nu^+\mathbf{Y}_\nu)_{ij}$ is given by eq.(50). In particular $(\mathbf{Y}_\nu^+\mathbf{Y}_\nu)_{21}$ is given by eq.(53)

$$(\mathbf{Y}_\nu^+\mathbf{Y}_\nu)_{21} = \mathcal{M} [U_{21}U_{11}^*(\kappa_1 - \kappa_2)] = |Y_0|^2 U_{21}U_{11}^* \frac{\Delta\kappa_{sol}^2}{\kappa^2} . \quad (61)$$

where, again, $|Y_0|^2 \simeq \mathcal{M}\kappa$ is the largest eigenvalue of $\mathbf{Y}_\nu^+\mathbf{Y}_\nu$. This equation is identical to eq.(60), multiplied by $\kappa^{-2}\sqrt{\Delta\kappa_{sol}^2\Delta\kappa_{atm}^2}$. This is a factor $\sim 10^{-4}$ for the LAMSW. Therefore all the plots representing $\text{BR}(\mu \rightarrow e, \gamma)$ in the previous scenario (Fig. 9) are valid here, but with the vertical axis re-scaled eight orders of magnitude smaller. Consequently, $\text{BR}(\mu \rightarrow e, \gamma)$ is naturally suppressed below the present (and even forthcoming) limits.

- If R is complex, $\mathbf{Y}_\nu^+\mathbf{Y}_\nu$ is given by eq.(54), which may have sizeable off-diagonal entries. Hence, $\text{BR}(\mu \rightarrow e, \gamma)$, could be very large in this case.
- If the (quasi-) degeneracy is only partial: $\kappa_3 \ll \kappa_1 \simeq \kappa_2 \equiv \kappa \sim \sqrt{\Delta\kappa_{atm}^2}$, $(\mathbf{Y}_\nu^+\mathbf{Y}_\nu)_{21}$ is given (for R real) by eq.(55). Again, this equation is identical to eq.(60), multiplied now by $\sqrt{\frac{\Delta\kappa_{sol}^2}{\Delta\kappa_{atm}^2}}$. This represents a suppression factor $\sim 10^{-1}$ for the LAMSW, which means that all the plots representing $\text{BR}(\mu \rightarrow e, \gamma)$ are as those of Fig. 9, re-scaled by a factor $\sim 10^{-2}$. As a consequence, $\text{BR}(\mu \rightarrow e, \gamma)$ for this partially degenerate scenario should be testable within the next generation of experiments. The conclusion is similar for $\text{BR}(\tau \rightarrow \mu, \gamma)$.

For generic complex R , the value of $\text{BR}(\mu \rightarrow e, \gamma)$ does not get any suppression and falls naturally above the present experimental limits.

6 Concluding remarks

If the origin of the neutrino masses is a supersymmetric see-saw, which is probably the most attractive scenario to explain their smallness, then the leptonic soft breaking

terms acquire off-diagonal contributions through the RG running, which drive non-vanishing $\text{BR}(l_i \rightarrow l_j, \gamma)$. These contributions are proportional to $(\mathbf{Y}_\nu^\dagger \mathbf{Y}_\nu)_{ij}$, where \mathbf{Y}_ν is the neutrino Yukawa matrix,

Therefore, in order to make predictions for these branching ratios, one has first to determine the most general form of \mathbf{Y}_ν and $\mathbf{Y}_\nu^\dagger \mathbf{Y}_\nu$, compatible with all the phenomenological requirements. This has been the first task of this paper, and the result is summarized in eqs.(13, 14).

Then, we have shown that the predictions for $\text{BR}(\mu \rightarrow e, \gamma)$ are normally *above* the *present* experimental limits if the three following conditions occur

1. The solution to the solar neutrino problem is the LAMSW, as favoured by the most recent analyses.
2. $Y_0(M_X) = \mathcal{O}(1)$, where $|Y_0|^2$ is the largest eigenvalue of $(\mathbf{Y}_\nu^\dagger \mathbf{Y}_\nu)$. This occurs e.g. in most grand-unified scenarios.
3. The soft-breaking terms are generated at a high-energy scale, e.g. M_X , above the Majorana mass of the right-handed neutrinos, M .

These conditions are very plausible. In our opinion, the most natural scenarios fulfill them, but certainly there exists other possibilities. E.g. concerning condition 1, the solution to the solar neutrino problem could be LOW. In this case, $\text{BR}(\mu \rightarrow e, \gamma)$ is (~ 20 times) smaller, but still testable in the forthcoming experiments. Condition 2 is satisfied in $SO(10)$ models, but it could be unfulfilled in $SU(5)$ models or in string scenarios with no GUT group. Still, we have noted in this work that even for $Y_0 = \mathcal{O}(10^{-1})$, most of the parameter space will be probed in the forthcoming generation of experiments (year 2003). Finally, condition 3 seems a natural one, as the see-saw mechanism requires the existence of high-energy scales, and it is hardly compatible e.g. with models where the fundamental scale is \mathcal{O} (TeV). Actually, if the initial scale at which universality is imposed is larger than the ordinary GUT M_X scale (as it is common in gravity mediated supersymmetry breaking), the predictions for the branching ratios increase. However, it may happen that supersymmetry is broken at a scale below M . This is the case of gauge-mediated scenarios, where there would be no generation of off-diagonal leptonic soft terms through the RG running. In this sense,

the gauge-mediated models are free from $\mu \rightarrow e, \gamma$ constraints and represent a way-out to the previous conclusion.

Even under the previous 1–3 conditions, there are physical scenarios compatible with the present $\text{BR}(\mu \rightarrow e, \gamma)$ experimental limits. Namely

- Whenever all the leptonic flavour violation can be attributed to the sector of right-handed neutrinos. This happens when there exists a basis in which the gauge couplings, \mathbf{Y}_e and \mathbf{Y}_ν get simultaneously flavour-diagonal, while the right-handed Majorana matrix, \mathcal{M} , gets non-diagonal. In this case there is no RG generation of non-diagonal soft terms, and the predictions for $\text{BR}(l_i \rightarrow l_i, \gamma)$ are as in the SM, i.e. negligible.

This possibility certainly exists and might be considered an attractive one. However, it should be noticed that it does *not* occur in the quark sector since the \mathbf{Y}_u and \mathbf{Y}_d Yukawa matrices cannot be simultaneously diagonalized in a basis where the gauge couplings remain diagonal. In our opinion, it would be a big chance that this happens in the leptonic sector.

- In the scenario where both, the left-handed and the right-handed neutrinos have hierarchical masses, there are two special textures, shown in eqs.(39, 40), where $\text{BR}(\mu \rightarrow e, \gamma)$ becomes suppressed. The first one is probably the most appealing, since it takes place for the simple case $R = \mathbf{1}$ in eq.(13). This is equivalent to assume that there exists a basis of L_i and ν_{Ri} in which \mathbf{Y}_ν and \mathcal{M} are simultaneously diagonal, though not \mathbf{Y}_e . In other words, all the leptonic flavour violation can be attributed to the sector of charged leptons.

Then, we have shown that for this privileged texture $\text{BR}(\tau \rightarrow \mu, \gamma)$ is not suppressed, lying in general above the forthcoming experimental upper bound.

- If the left-handed neutrinos are quasi-degenerate, then $\text{BR}(l_i \rightarrow l_j, \gamma)$ are naturally suppressed. Namely, if the R matrix in eq.(13) is real, there is a GIM-like mechanism that drives $\text{BR}(l_i \rightarrow l_j, \gamma)$ below the experimental limits, even the forthcoming ones. (This is not the case, however, if R is complex.)

If the degeneracy is partial (case of inverse hierarchy of neutrino masses), $\text{BR}(\mu \rightarrow e, \gamma)$ is somewhat suppressed, but still testable in the forthcoming experiments. The latter is also true for $\text{BR}(\tau \rightarrow \mu, \gamma)$

In our opinion, if the above 1–3 conditions are fulfilled, the scenario of quasi-degenerate neutrinos and the one with gauge mediated supersymmetry breaking represent the most plausible explanations to the absence of $\mu \rightarrow e, \gamma$ observations, specially if the absence persists after the next generation of experiments.

As a final conclusion, the discovery of neutrino oscillations makes much more plausible the possibility of observing lepton-flavour-violation processes, specially $\mu \rightarrow e, \gamma$, if the theory is supersymmetric and the neutrino masses are generated by a see-saw mechanism. Large regions of the parameter space are *already excluded* on these grounds, and there exists great chances to observe $\mu \rightarrow e, \gamma$ in the near future (PSI, 2003). This means that, hopefully, we will have signals of supersymmetry before LHC.

Acknowledgements

The work of J.A.C. was supported in part by the CICYT (contract AEN98-0816). A.I. would like to thank JoAnne Hewett and Gudrun Hiller, and specially Sacha Davidson and Graham Ross for very interesting discussions and invaluable suggestions. A.I. would also like to thank the SLAC theory group for hospitality during the first stages of this work.

Appendix

In the appendix, we summarize the relevant formulas concerning RGEs and the coefficients of the amplitude appearing in eq.(27).

Between M_X and M the evolution of the Yukawa couplings is given by

$$\frac{d\mathbf{Y}_\nu}{dt} = -\frac{1}{16\pi^2}\mathbf{Y}_\nu \left[\left(3g_2^2 + \frac{3}{5}g_1^2 - T_2 \right) \mathbf{I}_3 - \left(3\mathbf{Y}_\nu^+\mathbf{Y}_\nu + \mathbf{Y}_e^+\mathbf{Y}_e \right) \right], \quad (62)$$

$$\frac{d\mathbf{Y}_e}{dt} = -\frac{1}{16\pi^2}\mathbf{Y}_e \left[\left(3g_2^2 + \frac{9}{5}g_1^2 - T_1 \right) \mathbf{I}_3 - \left(\mathbf{Y}_\nu^+\mathbf{Y}_\nu + 3\mathbf{Y}_e^+\mathbf{Y}_e \right) \right], \quad (63)$$

$$\frac{d\mathbf{Y}_U}{dt} = -\frac{1}{16\pi^2}\mathbf{Y}_U \left[\left(\frac{13}{15}g_1^2 + 3g_2^2 + \frac{16}{3}g_3^2 - T_2 \right) \mathbf{I}_3 - 3\mathbf{Y}_U^+\mathbf{Y}_U - \mathbf{Y}_D^+\mathbf{Y}_D \right], \quad (64)$$

where

$$T_1 = \text{Tr}(3\mathbf{Y}_D^+\mathbf{Y}_D + \mathbf{Y}_e^+\mathbf{Y}_e), \quad T_2 = \text{Tr}(3\mathbf{Y}_U^+\mathbf{Y}_U + \mathbf{Y}_\nu^+\mathbf{Y}_\nu), \quad (65)$$

and

$$\frac{d\mathcal{M}}{dt} = \frac{1}{8\pi^2} \left[\mathcal{M}(\mathbf{Y}_\nu \mathbf{Y}_\nu^\dagger)^T + \mathbf{Y}_\nu \mathbf{Y}_\nu^\dagger \mathcal{M} \right]; \quad (66)$$

The renormalization group equations for the soft masses and trilinear terms are:

$$\begin{aligned} \frac{d\mathbf{m}_L^2}{dt} = & \frac{1}{16\pi^2} \left[(\mathbf{m}_L^2 \mathbf{Y}_e^\dagger \mathbf{Y}_e + \mathbf{Y}_e^\dagger \mathbf{Y}_e \mathbf{m}_L^2) + (\mathbf{m}_L^2 \mathbf{Y}_\nu^\dagger \mathbf{Y}_\nu + \mathbf{Y}_\nu^\dagger \mathbf{Y}_\nu \mathbf{m}_L^2) \right. \\ & + 2(\mathbf{Y}_e^\dagger \mathbf{m}_e^2 \mathbf{Y}_e + m_{H_1}^2 \mathbf{Y}_e^\dagger \mathbf{Y}_e + \mathbf{A}_e^\dagger \mathbf{A}_e) + 2(\mathbf{Y}_\nu^\dagger \mathbf{m}_\nu^2 \mathbf{Y}_\nu + m_{H_2}^2 \mathbf{Y}_\nu^\dagger \mathbf{Y}_\nu + \mathbf{A}_\nu^\dagger \mathbf{A}_\nu) \\ & \left. - \left(\frac{6}{5} g_1^2 |M_1|^2 + 6g_2^2 |M_2|^2 \right) \mathbf{I}_3 - \frac{3}{5} g_1^2 S \mathbf{I}_3 \right], \end{aligned} \quad (67)$$

$$\begin{aligned} \frac{d\mathbf{m}_e^2}{dt} = & \frac{1}{16\pi^2} \left[2(\mathbf{m}_e^2 \mathbf{Y}_e \mathbf{Y}_e^\dagger + \mathbf{Y}_e \mathbf{Y}_e^\dagger \mathbf{m}_e^2) + 4(\mathbf{Y}_e \mathbf{m}_L^2 \mathbf{Y}_e^\dagger + m_{H_1}^2 \mathbf{Y}_e \mathbf{Y}_e^\dagger + \mathbf{A}_e \mathbf{A}_e^\dagger) \right. \\ & \left. - \frac{24}{5} g_1^2 |M_1|^2 \mathbf{I}_3 + \frac{6}{5} g_1^2 S \mathbf{I}_3 \right], \end{aligned} \quad (68)$$

$$\frac{d\mathbf{m}_\nu^2}{dt} = \frac{1}{16\pi^2} \left[2(\mathbf{m}_\nu^2 \mathbf{Y}_\nu \mathbf{Y}_\nu^\dagger + \mathbf{Y}_\nu \mathbf{Y}_\nu^\dagger \mathbf{m}_\nu^2) + 4(\mathbf{Y}_\nu \mathbf{m}_L^2 \mathbf{Y}_\nu^\dagger + m_{H_2}^2 \mathbf{Y}_\nu \mathbf{Y}_\nu^\dagger + \mathbf{A}_\nu \mathbf{A}_\nu^\dagger) \right], \quad (69)$$

$$\begin{aligned} \frac{dm_{H_2}^2}{dt} = & \frac{1}{16\pi^2} \left[6\text{Tr}(\mathbf{Y}_U^\dagger (\mathbf{m}_Q^2 + \mathbf{m}_U^2 + m_{H_2}^2 \mathbf{I}_3) \mathbf{Y}_U + \mathbf{A}_U^\dagger \mathbf{A}_U) \right. \\ & + 2\text{Tr}(\mathbf{Y}_\nu^\dagger (\mathbf{m}_L^2 + \mathbf{m}_\nu^2 + m_{H_2}^2 \mathbf{I}_3) \mathbf{Y}_\nu + \mathbf{A}_\nu^\dagger \mathbf{A}_\nu) \\ & \left. - \left(\frac{6}{5} g_1^2 |M_1|^2 + 6g_2^2 |M_2|^2 \right) + \frac{3}{5} g_1^2 S \right], \end{aligned} \quad (70)$$

$$\begin{aligned} \frac{d\mathbf{A}_e}{dt} = & \frac{1}{16\pi^2} \left[\left\{ -\frac{9}{5} g_1^2 - 3g_2^2 + 3\text{Tr}(\mathbf{Y}_D^\dagger \mathbf{Y}_D) + \text{Tr}(\mathbf{Y}_e^\dagger \mathbf{Y}_e) \right\} \mathbf{A}_e \right. \\ & + 2 \left\{ -\frac{9}{5} g_1^2 M_1 - 3g_2^2 M_2 + 3\text{Tr}(\mathbf{Y}_D^\dagger \mathbf{A}_D) + \text{Tr}(\mathbf{Y}_e^\dagger \mathbf{A}_e) \right\} \mathbf{Y}_e \\ & \left. + 4(\mathbf{Y}_e \mathbf{Y}_e^\dagger \mathbf{A}_e) + 5(\mathbf{A}_e \mathbf{Y}_e^\dagger \mathbf{Y}_e) + 2(\mathbf{Y}_e \mathbf{Y}_\nu^\dagger \mathbf{A}_\nu) + (\mathbf{A}_e \mathbf{Y}_\nu^\dagger \mathbf{Y}_\nu) \right], \end{aligned} \quad (71)$$

$$\begin{aligned} \frac{d\mathbf{A}_\nu}{dt} = & \frac{1}{16\pi^2} \left[\left\{ -\frac{3}{5} g_1^2 - 3g_2^2 + 3\text{Tr}(\mathbf{Y}_U^\dagger \mathbf{Y}_U) + \text{Tr}(\mathbf{Y}_\nu^\dagger \mathbf{Y}_\nu) \right\} \mathbf{A}_\nu \right. \\ & + 2 \left\{ -\frac{3}{5} g_1^2 M_1 - 3g_2^2 M_2 + 3\text{Tr}(\mathbf{Y}_U^\dagger \mathbf{A}_U) + \text{Tr}(\mathbf{Y}_\nu^\dagger \mathbf{A}_\nu) \right\} \mathbf{Y}_\nu \\ & \left. + 4(\mathbf{Y}_\nu \mathbf{Y}_\nu^\dagger \mathbf{A}_\nu) + 5(\mathbf{A}_\nu \mathbf{Y}_\nu^\dagger \mathbf{Y}_\nu) + 2(\mathbf{Y}_\nu \mathbf{Y}_e^\dagger \mathbf{A}_e) + (\mathbf{A}_\nu \mathbf{Y}_e^\dagger \mathbf{Y}_e) \right], \end{aligned} \quad (72)$$

$$\begin{aligned} \frac{d\mathbf{A}_U}{dt} = & \frac{1}{16\pi^2} \left[\left\{ -\frac{13}{15} g_1^2 - 3g_2^2 - \frac{16}{3} g_3^2 + 3\text{Tr}(\mathbf{Y}_U^\dagger \mathbf{Y}_U) + \text{Tr}(\mathbf{Y}_\nu^\dagger \mathbf{Y}_\nu) \right\} \mathbf{A}_U \right. \\ & + 2 \left\{ -\frac{13}{15} g_1^2 M_1 - 3g_2^2 M_2 - \frac{16}{3} g_3^2 M_3 + 3\text{Tr}(\mathbf{Y}_U^\dagger \mathbf{A}_U) + \text{Tr}(\mathbf{Y}_\nu^\dagger \mathbf{A}_\nu) \right\} \mathbf{Y}_U \\ & \left. + 4(\mathbf{Y}_U \mathbf{Y}_U^\dagger \mathbf{A}_U) + 5(\mathbf{A}_U \mathbf{Y}_U^\dagger \mathbf{Y}_U) + 2(\mathbf{Y}_U \mathbf{Y}_D^\dagger \mathbf{A}_D) + (\mathbf{A}_U \mathbf{Y}_D^\dagger \mathbf{Y}_D) \right], \end{aligned} \quad (73)$$

where

$$S = \text{Tr}(\mathbf{m}_Q^2 + \mathbf{m}_d^2 - 2\mathbf{m}_u^2 - \mathbf{m}_L^2 + \mathbf{m}_e^2) - m_{H_1}^2 + m_{H_2}^2. \quad (74)$$

Here g_2 and g_1 are the $SU(2)_L$ and $U(1)_Y$ gauge coupling constants, and $\mathbf{Y}_{U,D,e,\nu}$ are the Yukawa matrices for up quarks, down quarks, charged leptons and neutrinos

respectively. The RGEs for \mathbf{Y}_D and the rest of the soft masses or trilinear terms are the same as in the MSSM. Below M , the RGEs are the same, except that the right neutrinos decouple, and hence \mathbf{Y}_ν disappears from the equations.

On the other hand, following ref.[9] the amplitude for the process $l_i \rightarrow l_j \gamma$ can be written as

$$T = \epsilon^\alpha \bar{l}_j m_{l_i} i \sigma_{\alpha\beta} q^\beta (A_L P_L + A_R P_R) l_i, \quad (75)$$

$$A_{L,R} = A_{L,R}^{(c)} + A_{L,R}^{(n)}$$

$$A_L^{(c)} = -\frac{e}{16\pi^2} \frac{1}{m_{\tilde{\nu}_X}^2} \left[C_{jAX}^L C_{iAX}^{L*} I_1(M_{\tilde{\chi}_A^-}^2/m_{\tilde{\nu}_X}^2) + C_{jAX}^L C_{iAX}^{R*} \frac{M_{\tilde{\chi}_A^-}}{m_{l_i}} I_1(M_{\tilde{\chi}_A^-}^2/m_{\tilde{\nu}_X}^2) \right] \quad (76)$$

$$A_L^{(n)} = \frac{e}{16\pi^2} \frac{1}{m_{\tilde{l}_X}^2} \left[N_{jAX}^L N_{iAX}^{L*} J_1(M_{\tilde{\chi}_A^0}^2/m_{\tilde{l}_X}^2) + N_{jAX}^L N_{iAX}^{R*} \frac{M_{\tilde{\chi}_A^0}}{m_{l_i}} J_2(M_{\tilde{\chi}_A^0}^2/m_{\tilde{l}_X}^2) \right], \quad (77)$$

$$A_R^{(c,n)} = A_L^{(c,n)}|_{L \leftrightarrow R}, \quad (78)$$

where $M_{\tilde{\chi}_A^-} (M_{\tilde{\chi}_A^0})$ is the chargino (neutralino) mass and $m_{\tilde{\nu}_X}^2 (m_{\tilde{l}_X}^2)$ is the sneutrino (charged slepton) mass squared.

The functions $I_{1,2}$ and $J_{1,2}$ are defined as follows:

$$I_1(r) = \frac{1}{12(1-r)^4} (2 + 3r - 6r^2 + r^3 + 6r \ln r), \quad (79)$$

$$I_2(r) = \frac{1}{2(1-r)^3} (-3 + 4r - r^2 - 2 \ln r), \quad (80)$$

$$J_1(r) = \frac{1}{12(1-r)^4} (1 - 6r + 3r^2 + 2r^3 - 6r^2 \ln r), \quad (81)$$

$$J_2(r) = \frac{1}{2(1-r)^3} (1 - r^2 + 2r \ln r), \quad (82)$$

Finally,

$$C_{iAX}^R = -g_2 (O_R)_{A1} U_{X,i}^\nu, \quad (83)$$

$$C_{iAX}^L = g_2 \frac{m_{l_i}}{\sqrt{2} m_W \cos \beta} (O_L)_{A2} U_{X,i}^\nu, \quad (84)$$

where $A = 1, 2$ and $X = 1, 2, 3$, and

$$N_{iAX}^R = -\frac{g_2}{\sqrt{2}} \{ [-(O_N)_{A2} - (O_N)_{A1} \tan \theta_W] U_{X,i}^l + \frac{m_{l_i}}{m_W \cos \beta} (O_N)_{A3} U_{X,i+3}^l \}, \quad (85)$$

$$N_{iAX}^L = -\frac{g_2}{\sqrt{2}} \{ \frac{m_{l_i}}{m_W \cos \beta} (O_N)_{A3} U_{X,i}^l + 2(O_N)_{A1} \tan \theta_W U_{X,i+3}^l \}, \quad (86)$$

where $A = 1, \dots, 4$ and $X = 1, \dots, 6$. The different matrices in these equations are defined in Appendix B of ref.[9].

References

- [1] Y. Fukuda *et al.* [Super-Kamiokande Collaboration], Phys. Rev. Lett. **81** (1998) 1562; Phys. Rev. Lett. **82** (1999) 1810. Phys. Rev. Lett. **82** (1999) 2430; Phys. Rev. Lett. **77** (1996) 1683; S. Hatakeyama *et al.* [Kamiokande Collaboration], Phys. Rev. Lett. **81** (1998) 2016; W. W. Allison *et al.*, Phys. Lett. B **391** (1997) 491; W. W. Allison *et al.* [Soudan-2 Collaboration], Phys. Lett. B **449** (1999) 137; B.T. Cleveland *et al.*, Homestake Collaboration, Astrophys. J. **496** (1998) 505; W. Hampel *et al.* [GALLEX Collaboration], Phys. Lett. B **388** (1996) 384. D. N. Abdurashitov *et al.*, Phys. Rev. Lett. **77** (1996) 4708.
- [2] S. M. Bilenkii, S. T. Petcov and B. Pontecorvo, Phys. Lett. B **67** (1977) 309; T. P. Cheng and L. Li, Phys. Rev. Lett. **45** (1980) 1908; W. J. Marciano and A. I. Sanda, Phys. Lett. B **67** (1977) 303; B. W. Lee, S. Pakvasa, R. E. Shrock and H. Sugawara, Phys. Rev. Lett. **38** (1977) 937 [Erratum-ibid. **38** (1977) 937].
- [3] S. Dimopoulos and H. Georgi, Nucl. Phys. B **193** (1981) 150. J. Ellis and D.V. Nanopoulos, Phys. Lett. B **110** (1982) 44; R. Barbieri and R. Gatto, Phys. Lett. B **110** (1982) 211; M. Duncan, Nucl. Phys. B **221** (1983) 285; J. Donoghue, H.P. Nilles and D. Wyler, Phys. Lett. B **128** (1983) 55; A. Bouquet, J. Kaplan and C.A. Savoy, Phys. Lett. B **148** (1984) 69; L. Hall, V. Kostelecky and S. Raby, Nucl. Phys. B **267** (1986) 415.
- [4] F. Gabbiani and A. Masiero, Nucl. Phys. B **322** (1989) 235; J.S. Hagelin, S. Kelley and T. Tanaka, Nucl. Phys. B **415** (1994) 293; D. Choudhury, F. Eberlein, A. König, J. Louis and S. Pokorski, Phys. Lett. B **342** (1995) 180; P. Brax and M. Chemtob, Phys. Rev. D **51** (1995) 6550; P. Brax and C. A. Savoy, Nucl. Phys. B **447** (1995) 227; R. Barbieri and L.J. Hall, Phys. Lett. B **338** (1994) 212; B. de Carlos, J. A. Casas and J. M. Moreno, Phys. Rev. D **53** (1996) 6398; I. Lee, Nucl. Phys. B **246** (1984) 120; I. Lee, Phys. Lett. B **138** (1984) 121.
- [5] M. Gell-Mann, P. Ramond and R. Slansky, proceedings of the Supergravity Stony Brook Workshop, New York, 1979, eds. P. Van Nieuwenhuizen and D. Freedman (North-Holland, Amsterdam); T. Yanagida, proceedings of the Workshop on Unified Theories and Baryon Number in the Universe, Tsukuba, Japan 1979 (edited

- by A. Sawada and A. Sugamoto, KEK Report No. 79-18, Tsukuba); R. Mohapatra and G. Senjanović, *Phys. Rev. Lett.* **44** (1980) 912, *Phys. Rev.* **D23** (1981) 165.
- [6] F. Borzumati and A. Masiero, *Phys. Rev. Lett.* **57** (1986) 961.
- [7] J. A. Casas, V. Di Clemente, A. Ibarra and M. Quiros, *Phys. Rev. D* **62** (2000) 053005.
- [8] J. Ellis, M. E. Gomez, G. K. Leontaris, S. Lola and D. V. Nanopoulos, *Eur. Phys. J. C* **14** (2000) 319; M. E. Gomez, G. K. Leontaris, S. Lola and J. D. Vergados, *Phys. Rev. D* **59** (1999) 116009; J. L. Feng, Y. Nir and Y. Shadmi, *Phys. Rev. D* **61** (2000) 113005. G. K. Leontaris and N. D. Tracas, *Phys. Lett. B* **431** (1998) 90; W. Buchmuller, D. Delepine and L. T. Handoko, *Nucl. Phys. B* **576** (2000) 445. W. Buchmuller, D. Delepine and F. Vissani, *Phys. Lett. B* **459** (1999) 171; D. F. Carvalho, M. E. Gomez and S. Khalil, hep-ph/0101250; J. Sato and K. Tobe, hep-ph/0012333; S. F. King and M. Oliveira, *Phys. Rev. D* **60** (1999) 035003; R. Barbieri, L. Hall and A. Strumia, *Nucl. Phys. B* **445** (1995) 219.
- [9] J. Hisano, T. Moroi, K. Tobe and M. Yamaguchi, *Phys. Rev. D* **53** (1996) 2442.
- [10] J. Hisano and D. Nomura, *Phys. Rev. D* **59** (1999) 116005.
- [11] J. Sato, K. Tobe and T. Yanagida, *Phys. Lett. B* **498** (2001) 189.
- [12] J. Hisano, D. Nomura, Y. Okada, Y. Shimizu and M. Tanaka, *Phys. Rev. D* **58** (1998) 116010; J. Hisano, D. Nomura and T. Yanagida, *Phys. Lett. B* **437** (1998) 351; J. Hisano, T. Moroi, K. Tobe and M. Yamaguchi, *Phys. Lett. B* **391** (1997) 341; P. Ciafaloni, A. Romanino and A. Strumia, *Nucl. Phys. B* **458** (1996) 3; G. Barenboim, K. Huitu and M. Raidal, *Phys. Rev. D* **63** (2001) 055006;
- [13] Z. Maki, M. Nakagawa and S. Sakata, *Prog. Theor. Phys.* **28** (1962) 870.
- [14] See e.g. R. N. Mohapatra, “Supersymmetric grand unification: An update,” hep-ph/9911272.
- [15] Y. Kuno and Y. Okada, *Phys. Rev. Lett.* **77** (1996) 434; Y. Kuno, A. Maki and Y. Okada, *Phys. Rev. D* **55** (1997) 2517.
- [16] M. L. Brooks *et al.* [MEGA Collaboration], *Phys. Rev. Lett.* **83** (1999) 1521.

- [17] L. M. Barkov et al., Research Proposal for an experiment at PSI (1999). See the webpage: <http://meg.psi.ch/>.
- [18] S. Ahmed *et al.* [CLEO Collaboration], Phys. Rev. D **61** (2000) 071101.
- [19] See Ellis et al. in ref.[6].
- [20] U. Bellgardt et al., Nucl. Phys. B229 (1988) 1.
- [21] P. Wintz, *Proceedings of the First International Symposium on Lepton and Baryon Number Violation*, eds. H.V. Klapdor-Kleingrothaus and I.V. Krivosheina (Institute of Physics, Bristol, 1998), p.534.
- [22] M. Bachmann et al., MECO collaboration, Research Proposal E940 for an experiment at BNL (1997).
- [23] See for example Y. Kuno and Y. Okada, hep-ph/9909265.
- [24] See e.g. M. C. Gonzalez-Garcia, M. Maltoni, C. Pena-Garay and J. W. Valle, Phys. Rev. D **63** (2001) 033005.
- [25] B. Pontecorvo, Sov. Phys. JETP**26** (1968) 984.
- [26] S. P. Mikheev and A. Y. Smirnov, Sov. J. Nucl. Phys. **42** (1985) 913; L. Wolfenstein, Phys. Rev. D **17** (1978) 2369.
- [27] G. Altarelli and F. Feruglio, *Phys. Lett.* **B439** (1998) 112, *JHEP* **9811** (1998) 021 , and *Phys. Lett.* **B451** (1999) 388.
- [28] See for example H. Georgi and S. L. Glashow, Phys. Rev. D **61** (2000) 097301.
- [29] J. A. Casas, J. R. Espinosa, A. Ibarra and I. Navarro, Nucl. Phys. B **573** (2000) 652.